Developing Recombinant Overlapping Peptides of Prostate-Specific Antigen as Vaccine

Chan, Song San
Wolfson College
University of Oxford

A thesis submitted for the degree of
Master of Research
Michaelmas 2023

Table of Contents

Developing Recombinant Overlapping Peptides of Prostate-Specific Antigen as Vaccine

Chan, Song San
Wolfson College
University of Oxford

A thesis submitted for the degree of
Master of Research
Michaelmas 2023

Abstract

Immunotherapy has become a new approach for prostate cancer (PCa) due to its selectivity and efficacy. With immunogenic properties, PSA has been found to be overexpressed in PCa and its enzymatic activity enhances the growth and progression of PCa cells. Furthermore, dendritic cell (DC) based therapies against PSA have been approved for clinical use which makes PSA a desirable target for recombinant overlapping peptides (ROPs) vaccine development. Based on combining multiple T cell epitopes, ROPs involves identifying a set of overlapping amino acid sequences constituting a single-chain peptide representing the sequence of PSA. Between each overlapping region is an enzymatic cleavage site specific for cathepsin S which is a key protease located in endolysosomes of DC. This strategy harnesses DC's potential of priming both CD4+ and CD8+ naïve T cells by its ability to be presented by MHC class I and II molecules, triggering robust cell-mediated anti-tumour immunity.

This project aims to develop and optimise the process of ROP-PSA expression and purification, and subsequently study the mechanism of activation of DCs *in vitro* using dendritic cell line DC2.4 by cytokine array assays. Here we demonstrate the successful expression of ROP-PSA from *E. coli*, the solubilisation of the recombinant ROP-PSA protein in urea, sarkosyl and arginine, and purification of ROP-PSA from *E. coli* expression system, which was validated by SDS-PAGE and western blot. Biocompatibility and stability of the buffer were tested by viability assay *in vitro* with the cell line to optimise buffer proportion in medium before cytokine array. Upon endotoxin removal, the concentration of ROP-PSA was accurately measured by bicinchoninic acid (BCA) assay for the calculation of treatment dose. Cytokine profiles have shown cytokine and chemokine release (e.g. TNF-α and significantly from CC chemokine family) from DC2.4 after treatment with ROP-PSA in cytokine array. Cathepsin S digestion assay and mass spectrometry analysis concluded some cleavage at cathepsin specific linker. The project provides a strong foundation for *in vivo* preclinical murine studies.

Disclaimer

I confirm that the work presented in this thesis is entirely my own work, with the exception of data from LPS quantification assay which was conducted by Yuqian Ou, a PhD student from Jiang's lab and methods and data from mass spectrometry which was conducted and analysed by Dr Rod Chalk from Centre for Medicines Discovery, University of Oxford.

List of abbreviations

ADT – androgen deprivation therapy
APC – antigen-presenting cells
AWE – alive without events
BME – β-mercaptoethanol
CAR – chimeric antigen receptor
CLIP – class II-associated invariant chain peptide
DC – dendritic cells
DRE – digital rectal exam
ER – endoplasmic reticulum
GM-CSF – granulocyte-macrophage colony-stimulating factor
GnRH – gonadotropin-releasing hormone
HLA – human leukocyte antigen
Ii - invariant chain
mCRPC – metastatic castration-resistant prostate cancer
MHC – major histocompatibility complex
MIIC – MHC class II enriched compartment
MoDC – monocyte-derived dendritic cells
MTS – 3-(4,5-dimethylthiazol-2-yl)-5-(3-carboxymethoxyphenyl)-2-(4-sulfophenyl)-2H-tetrazolium
NK – natural killer (cells)
PAP – prostatic acid phosphatase
PBMC – peripheral blood mononuclear cells
PCa – prostate cancer
PCD – programmed cell death
PSA – prostate-specific antigen
PSMA – prostatic specific membrane antigen
ROP – recombinant overlapping peptides
SEER – surveillance, epidemiology, and end results
TAA – tumour-associated antigens
TCEP – tris(2-carboxyethyl)phosphine
TGF – tumour growth factor
TME – tumour microenvironment
TNM – tumour, node, metastasis
UPS – ubiquitin-proteasome system

Introduction

Prostate cancer

Prostate cancer (PCa) is the second most frequent malignancy in men (after lung cancer) and the fourth most commonly occurring cancer overall (1). In the UK, PCa is the second most common cause of cancer death in males (2). According to the data from the Surveillance, Epidemiology, and End Results (SEER) Program, the relative 5-year survival rate (2012-2018) for localized and regional PCa was 100% while it dropped to 32.3% when cancer had metastasized (3). It is highly likely to be cured of PCa when localized and current treatment can prolong survival in some metastasis such as bone (4). However, in most metastases, it cannot be cured by current treatment with median survival in between 1 and 3 years (4).

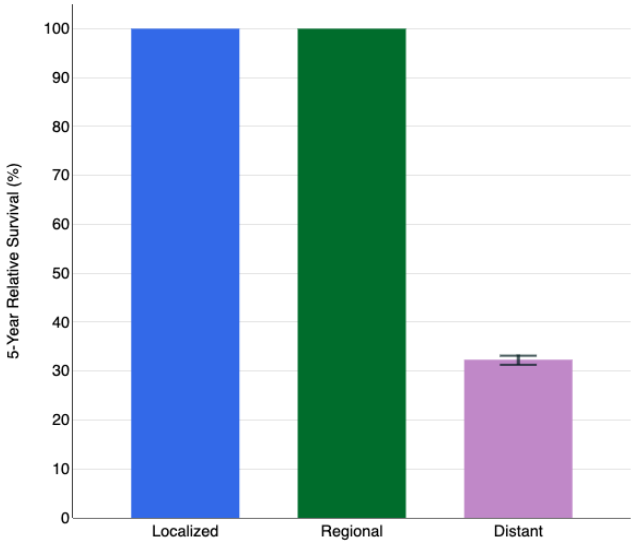

Figure 1 | 5-year relative survival rate for prostate cancer, 2012-2018. Source from National Cancer Institute.

Screening and Diagnosis

There is yet an efficient non-invasive method to diagnose prostate cancer. Although most prostate cancers are diagnosed as a results of screening, screening for prostate cancer remains controversial in the UK and even worldwide as it has yet been proved that the benefits would outweigh the risks in systemic reviews and meta-analysis (5)(6). According to robust evidence, available screening such as Prostate-Specific Antigen (PSA) tests and/or Digital Rectal Exam (DRE) can suggest false-positive result which leads to further unnecessary tests and treatments, some of which can be invasive and distressful (7,8). For example, adverse reactions caused by prostatic biopsies (a common diagnostic test) include fever, pain, haematuria, and rarely, sepsis (9). There is also solid evidence for how

overtreatment with radical prostatectomy and radiation therapy can lead to permanent adverse effects such as erectile dysfunction and urinary incontinence in many patients (10). Therefore, diagnosis may consider other factors such as clinical presentation and needle biopsy which is the most commonly used method.

Staging and Corresponding Treatment

Staging tests include serum PSA level, biopsy, pelvic lymph node dissection, imaging (e.g. MRI, transrectal ultrasound, CT, and radionuclide bone scans for metastases (4). Staging is mainly classified by TNM (tumour, node, metastasis) system (11). Treatment options for stage I to III local prostate cancers are heavily based on surgery, radiotherapy, and sometimes hormonal therapies (4). At Stage IV when tumour starts to spread to lymph nodes, apart from radical prostatectomy, hormonal therapies and bisphosphonates are used alone or in combination with radiotherapy (4). However, for recurrent metastatic prostate cancer, medical management is heavily used such as chemotherapy and immunotherapy (4).

Treatment options for recurrent/metastatic PCa

Hormonal therapy for PCa, commonly referred to as androgen deprivation therapy (ADT), forms the backbone of therapy for metastatic PCa, which can be fulfilled with bilateral orchiectomy or administration of gonadotropin-releasing hormone (GnRH) agonists or antagonists. 80-90% patients respond to treatment initially but majority of them develop advanced disease following ADT (12). It has been proved that combination therapy of ADT and hormonal agents (i.e. abiraterone, apalutamide and enzalutamide) results in longer overall survival than monotherapy (13–15).

Chemotherapy is often used as second-line when tumour becomes resistant to hormonal therapies. The most used chemotherapy agent is intravenous docetaxel. Combination with

docetaxel has been shown in randomized clinical trials to improve overall survival compared with monotherapy and not inferior to combination with hormonal therapy (16). Data published from ENZAMET trial showed superior PSA progression-free survival and clinical progression-free survival with the addition of enzalutamide (15). PEACE trial also indicated promising results on improving overall survival in triple therapy of chemotherapy, radiotherapy and hormonal therapy (17). With the principle of “hit hard, hit early” in cancer treatment, it is likely that triple therapy will become the new standard of care in PCa treatment (18).

Radium-223 can be used as combination therapy with ADT in bone metastases and can be effective for bone pain in patients (19). This radiopharmaceutical emits alpha particles and is administered by IV with a half-life of approximately 11 days (4).

Prognosis Factors

Overall survival for PCa patents are associated with several factors such as extent of tumour, histologic grade, patient’s age and health, and PSA level (4). As mentioned local tumours have high survival rates but not necessarily curable; there is no current treatment to cure metastatic PCa whose median survival rate is usually 1 to 3 years. Gleason score is a standardized method to measure the histologic grade of tumour and usually the less differentiated the tumours are, the more likely they would have metastasised before diagnosis (4). Elevation of PSA level and serum acid phosphatase levels is related to poor prognosis in both localized and metastasized PCa (4).

Immunotherapy for PCa

Immunotherapy in cancer harnesses the power of the immune system to kill cancer cells, by assisting the immune system to recognize and kill cancer cells. Immunotherapy is usually

used as final approach for PCa when disease progresses during ADT treatment (hormone-refractory). Immunogenicity of cancer vaccines requires time to develop and therefore not immediately cytotoxic and reduce tumour size as seen with chemotherapy or radiation (20).

The reasons why prostate cancer is suitable for immunotherapy are: 1. it progresses relatively slowly locally which allows sufficient time (21) for the immune system to develop efficient antitumour responses; 2. the tumour expresses several tumour-specific antigens e.g. PSA (22), prostatic acid phosphatase (PAP) (23) and prostatic specific membrane antigen (PSMA) (24) which are potential therapeutic targets; 3. targeting these antigens with prostate being a non-essential organ reduces the chance of causing acute off-target toxicities (25).

Development of dendritic cell-based vaccines in PCa

Antigen presentation is the key linkage between innate and adaptive immune system and fundamental to activate cytotoxic T lymphocytes for the induction of tumour apoptosis. The idea of cancer vaccines originated from random tumour regression following microbial infections (26). The efficacy of such therapeutics eventually requires the specific recognition of unique tumour-associated antigens (TAAs) by cytolytic effectors such as T cells and antibodies (27). One of the major hallmarks for PCa is immune invasion(28). Part of its reason is due to the immaturity and paucity of dendritic cells in the tumour, which contribute to non-immunogenic T cell responses at early stages and thus later stages (29,30). Therefore, a DC based immunotherapy may have a great potential to treat PCa.

Dendritic cells (DCs) as one of the primary professional antigen-presenting cells (APCs) act as a link between innate and adaptive immunity. They are innate immune cells for their function of recognizing and responding to pathogen-associated and damage associated

patterns and regulating inflammatory response (31). Their main role in adaptive immunity is defined by their ability to capture, process and express immunogenic antigens (32) via major histocompatibility complex (MHC) molecules to prime naïve T cells (31).

To overcome the low prevalence of DC in the peripheral blood (0.1%-1%) of peripheral blood mononuclear cells (PBMC) (33), Sipuleucel-T use a density gradient to prepare an APC enriched preparation(34). As DC therapy evolved, monocytes, which are a more readily available source (about 10% of PBMC), are used to be differentiated to dendritic-like cells (MoDC). In this case, CD14+ cells are extracted from PBMC and cultured with GM-CSF and IL-4 to stimulate the maturation and proliferation of MoDC (35). These cells are able to express internalised tumour antigen on major histocompatibility complex (MHC) I molecules (36). With their professional antigen-presenting ability, they induce T-cell maturation and proliferation (34).

First clinically approved PCa immunotherapy – Sipuleucel-T

Sipuleucel-T was the first immunotherapy approved by FDA for PCa personalised treatment, and it is also the first immunotherapy that is ever approved for cancer treatment. The recombinant protein is composed of both PAP and granulocyte-macrophage colony-stimulating factor (GM-CSF) which are a prominent tumour-associated antigen and a cytokine that help with T-cell and B-cell production and maturation, respectively. The product itself constitutes a recombinant fusion protein antigen which can be taken up by the patient's isolated APCs ex vivo obtained by leukapheresis (37), which result in APC activation (38). The mixture of cultured peripheral blood mononuclear cells with activated APCs is infused back into the patient (37). By expressing MHC class II-antigen and MHC class I-antigen complexes, these cells stimulate CD4+ T-helper cells and CD8+ cytotoxic cells, respectively, which activates T-cell immune response targeted against PAP (37). In phase III IMPACT

trial (placebo-controlled randomisation), the median overall survival was 4.1 months longer in sipuleucel-T than in the placebo group (39).

Clinical data showed that Sipuleucel-T could maintain prolonged peripheral T-cell and B-cell response to target antigen PAP, which then lead to downstream responses to secondary antigens i.e. antigen spread and T-cell infiltration to tumour tissue (40,41). Thus from various pathways, sipuleucel-T induces the activation of cytotoxic T lymphocytic activity and turn the immunosuppressive tumour microenvironment (TME) of PCa to an immune-enriched one (41,42). The landmark for Sipuleucel-T is its ability to prime cytotoxic T cells so that they become tumour-specific. This is beneficial in terms of combining with immune checkpoint inhibitor clinically as the presence of tumour-specific T-cells is the rate-limiting step for immune checkpoint blockade (43).

Form of antigen

Peptides and mRNA are the two main types of antigens for DC therapy.

Peptides

Cancer vaccine development usually originates from peptide or protein because it is the most common source of antigen (34). Synthetic peptide-based vaccines are usually well-tolerated and presents a satisfactory toxicity profile. In order to induce and stimulate antigen-specific tumour reactive T cells, these peptides should be able to be presented by human leukocyte antigen (HLA) molecules on APCs, which in turn prime CD4+ and CD8+ T cells (44). However its therapeutic effect often requires combination with robust adjuvants and immunomodulators (45) and largely depends on their specific suitability for patient's HLA subtype for antigen presentation (34). Peptides are easily produced, stored and does not require a "cold chain" for transportation, which makes manufacturing cost-effective (46).

Messenger RNA

mRNA has shown promise in recent years for the COVID-19 pandemic. By taking up and translating the mRNA, APCs, mostly dendritic cells, present/cross-present post-translated proteins, initiating immune response (47). mRNA can be administered to the DCs in four ways: passive, electroporation, lipid nanoparticles and viral vectors. Electroporation was used in an autologous DC therapy targeting PSA in a phase II trial for PCa; the therapy was proved to be safe (no significant adverse reactions) in all patients and immunogenic in half of the patients (48). Naked mRNA when injected directly into patients is rapidly degraded by extracellular RNases so development of delivery vehicles is necessary to increase the delivery efficiency of mRNA cancer vaccines (49). There is currently no clinically approved mRNA cancer immunotherapy.

Therapeutic vaccines compared with other immunotherapies

Apart from therapeutic vaccines, other immunotherapies such as immune checkpoint inhibitors, CAR (chimeric antigen receptor)-T cell, cytokines, and oncolytic viruses are widely used for cancer therapy nowadays. Immune checkpoint inhibitors and CAR-T cell therapies will be mainly discussed in this section. Immune checkpoint inhibitors target negative co-stimulatory molecules on cytotoxic and regulatory T-cells to prolong tumour-specific cytotoxic T cell response (1). However they can result in excessive autoimmune response e.g. rash, pneumonitis, and hepatitis which can confine their use (51). Also this therapy requires upregulation of immune checkpoints and the presence of tumour-specific T cells in TME (52) – clinical studies have shown limited response to this therapy by PCa patients given PCa is a “cold” tumour (53).

CAR-T cell therapies are a personalised immunotherapy. Through extracting the patient’s own T cells and engineering them with a tumour-specific surface molecule receptor i.e. CAR,

CAR-T cells are able to bind to cancer cells and induce cytotoxic T cell response (54). Despite its adverse reaction profile e.g. cytokine release syndrome and expensive cost, this therapy showed promising results in haematological cancers and most recently a PSMA-directed, tumour growth factor (TGF)-β-armoured CAR-T cell therapy demonstrated positive clinical activity in patients with castration-resistant prostate cancer (55).

Role of PSA in PCa immunotherapy

Therapeutic potential of PSA

PSA is a glycoprotein which can be overexpressed by prostate epithelial cells almost exclusively in the case of prostate abnormality, inflammation and trauma, or in this case, cancer, which enhances the amount of PSA in circulation (56). Therefore, PSA screening is widely used in the diagnosis of prostate cancer due to its simplicity while it has not been proved that the benefits would outweigh the risks as mentioned (6)(57). PSA has been found not purely a serum marker for diagnosis. PSA is also a clinically verified superb indicator for disease progression once cancer has been diagnosed. Moreover, it was shown to have a significant role in PCa signalling pathway for proliferation, angiogenesis and metastasis, which can facilitate tumour genesis and progression (58). In terms of immune response, PSA can give rise to the stimulation of TGFβ which is one of the major immune suppressive factors that orchestrate tumour evasion (59,60). HLA-A2-, HLA-A3- and HLA-A24-restricted PSA-derived peptides/epitopes from oligopeptides were reported to be able to activate CTLs and consequently lead to tumour apoptosis induced by peptide-specific CTLs (61), which makes PSA a potential target for PCa immunotherapy.

PSA-based vaccines under development

Dendritic cell-based vaccines with PSA as a target have entered clinical trials in the past. A vector-based vaccine against PSA-expressing tumour cells PSA-TRICOM, which

successfully reached phase III clinical trial, contain the transgene for PSA and three costimulatory molecules that can enhance PSA-specific T cell responses (TRICOM). It works under two pathways – with the infection of dendritic cells and somatic cells respectively. For pathway 1, the vaccinia virus harnesses the ability of DCs to express MHC class I/PSA epitopes to trigger the activation and proliferation of PSA-specific CD8+ T lymphocytes which induces programmed cell death (PCD) in tumour cells after circulating to tumour cells (62). For pathway 2 when somatic cells are infected by the vaccinia virus which induces the direct activation of PSA-specific CTLs, and natural killer (NK) cells which causes PCD in somatic cells. This mechanism harnesses the cross-presentation ability of DCs as dead somatic cells are engulfed by mature DCs and PSA cross-presented, which further stimulates PSA-specific CTL activation, inducing PCD of tumour cells (62).

In a phase I study, significant increase in CD4+ and CD8+ tumour infiltration has been shown in patients who were treatment naïve or recurrent after primary radiotherapy (63). At phase II, it demonstrated an 8.5-month improvement in median overall survival, in men with metastatic castration-resistant PCa (mCRPC) (64). At phase III trial in asymptomatic or minimally symptomatic mCRPC, Prostvac was proven to be safe and well tolerated. However it had shown no superior effects on overall survival and alive without events (AWE) compared to the placebo (65). Safe toxicity profile and in vivo immunogenicity in Prostvac allow opportunities for clinical trials with other therapeutic agents such as enzalutamide (nonsteroidal antiandrogen) (66), ipilimumab (CTLA-4 inhibitor) (67), and nivolumab (PD-1 inhibitor) (68). The immunotherapeutic combination of ipilimumab and Prostvac has shown early safety results in clinical studies (67).

Developing ROP-PSA as DC-based vaccine for PCa

Recombinant Overlapping Peptides (ROPs) are an innovative cancer vaccine strategy developed in our laboratory. This project aimed to develop an ROP which targets PSA as a tumour-associated antigen expressed by PCa.

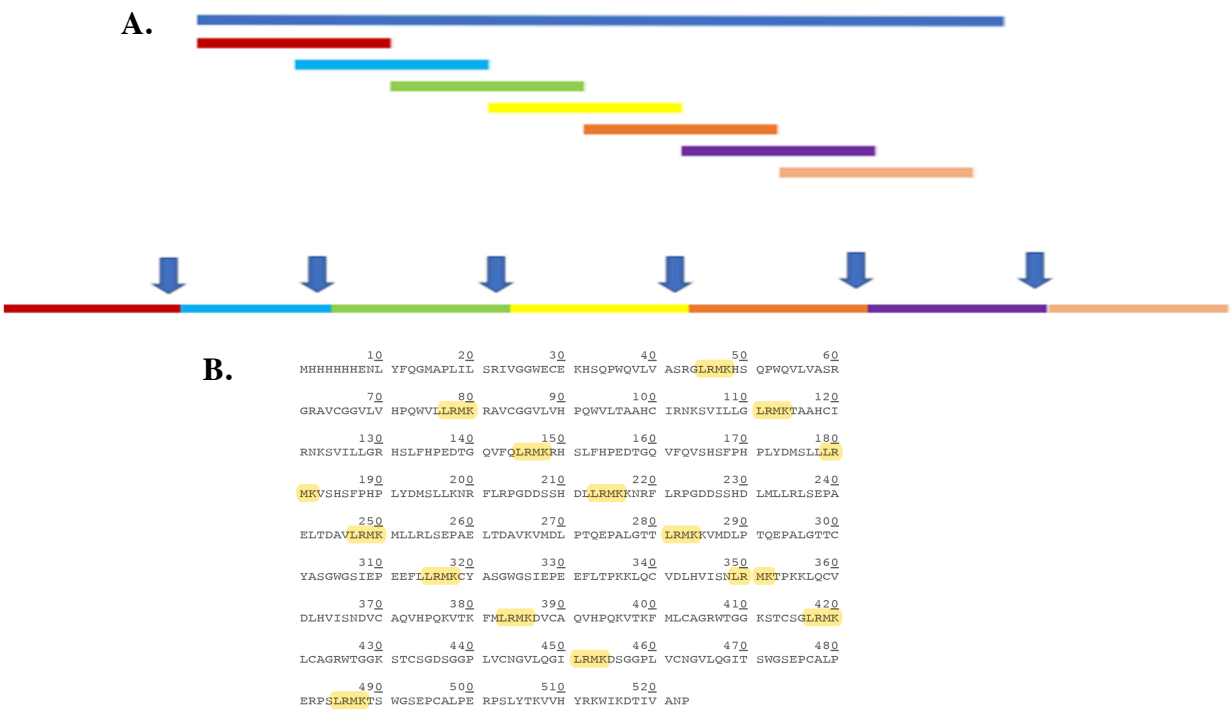

Figure 2 | (A) making ROP from single target protein. The top blue bar indicates the wild type PSA, while the multi-color bars represent recombinant overlapping peptides, being linked together by cathepsin S cleavage sites to form a long peptide sequence; **(B)** ROP-PSA protein (OVM300) with LRMK (cathepsin S cleavage sites) highlighted in yellow. Apart from the start and end ROP, an LRMK sequence is used to divide two 30-amino acid sequences.

Mechanism of action

Based on combining multiple T cell epitopes, the approach involves identifying a set of overlapping amino acid sequences constituting a single-chain peptide representing the sequence of PSA. The overlapping regions allow the possibility for epitope diversity and between each overlapping region is an enzymatic cleavage site specific for cathepsin S which is a key protease located in endolysosomes of DC, the professional antigen presenting cell linking innate and adaptive immune response. This strategy harnesses DC's potential of priming both CD4+ and CD8+ naïve T cells by its ability to be presented by MHC class I and II molecules, triggering robust cell-mediated anti-tumour immunity.

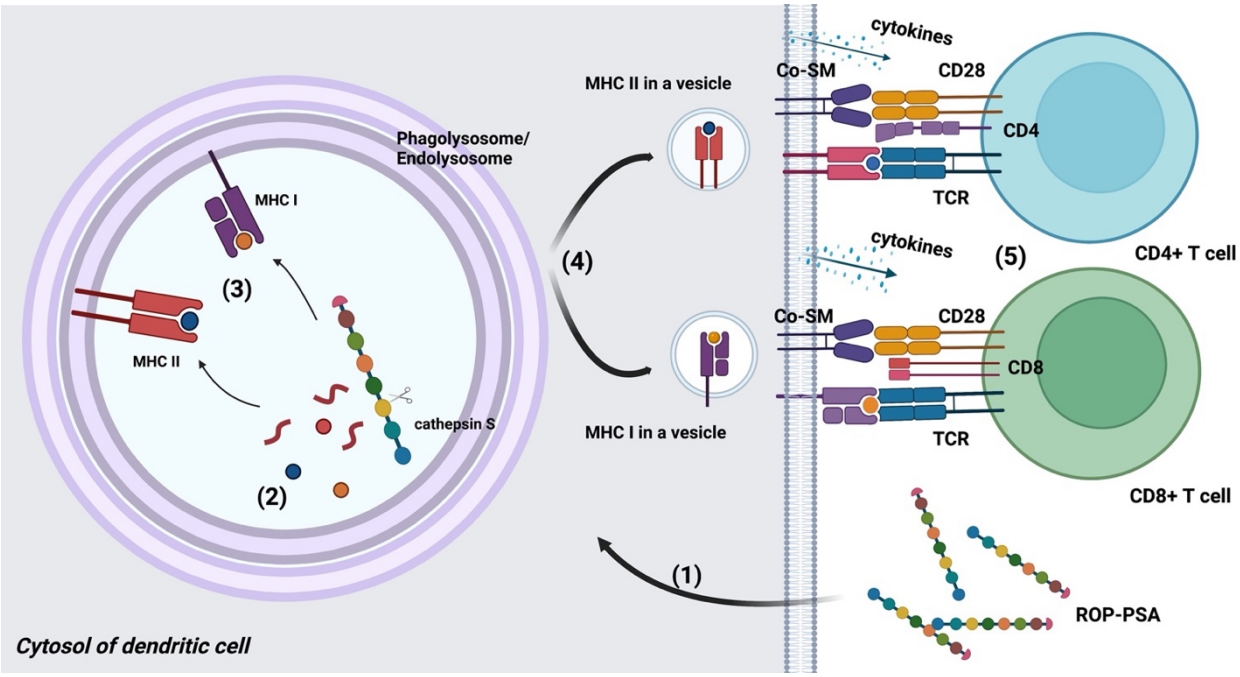

Figure 3 | Brief illustration of predicted mechanism of action of ROP-PSA created with BioRender.com. (1) Intact ROP-PSA is taken up by dendritic cells. (2) ROP-PSAs are digested by cathepsin S in endolysosome. (3) Antigen loading to MHC I and MHC II molecules. (4) Antigen-loaded MHC molecules are transported in vesicles to plasma membrane. (5) MHC II/peptide and MHC I/peptide complexes are presented and cross-presented to CD4+ T cell and CD8+ T cell on cell surface respectively to activate T cells. Costimulatory signals and cytokine release facilitate the survival and differentiation of T cells.

ROP-PSA presentation by MHC I and II molecules in dendritic cells

Dendritic cells are professional antigen presenting cells in the immune system which can present MHC I and II molecules to activate naïve CD8 T cells and CD4 T cells to become effector T cells. MHC II molecules are comprised of one α and one β chain which are

synthesized in the endoplasmic reticulum (ER) and stabilised by the invariant chain which is a chaperone molecule for the stabilisation of its structure(69). Cathepsin S is a cysteine endoprotease which recognizes LRMK sequence and regulates invariant chain (Ii) degradation in antigen-presenting cells (70). Digestion of Ii by cathepsin S facilitates the dissociation of class II-associated invariant chain peptide (CLIP) from MHC II, enabling antigen loading. After maturation, the heterotrimer (α/β/Ii) is translocated to MHC class II enriched compartment (MIIC), such as late endosome (69). Consequently, MHC II/peptide complexes move to cell membrane and are presented to T cell receptors of CD4+ T lymphocytes (69). MHC II proteins can contain and present peptides of 13-25 amino acids due to their open binding groove (71).

ROP utilises the exogenous pathway to cross present peptide fragments to the surface of some subsets of dendritic cells to stimulate CD8+ T cells. Upon phagocytosis, ROPs are expected to be processed by the cathepsin S in the endosome. In addition to the MHC class II pathway as mentioned above, some of the peptides are expected to bind to MHC I molecules in the cytosol by unknown mechanisms (72). There are two possible pathways being generally discussed: the vacuolar pathway and the cytosolic pathway. In vacuolar pathway, exogenous proteins are internalised via phagocytosis and digested by cathepsin S in endo/phagolysosomes where digested peptides are loaded onto MHC I molecules. ROPs are expected to be directly transported from the endolysosomes into a vesicular loading compartment (73,74), without passing through transporter associated with antigen processing (TAP) protein into the ER. Related evidence includes sensitivity to inhibitors of lysosomal proteolysis (75) and resistance to proteasome inhibitors (76). In summary, antigen loading can occur in both ER and endolysosome. MHC I proteins are only able to accommodate peptides of 8-10 amino acids as conserved tyrosine residues close the binding groove at both ends (71).

Cross presentation via the cytosolic pathway as the name suggests indicates engulfed proteins undergo degradation by the proteasome in the cytosol (76). It is hypothesized that ROPs enter this pathway through escaping endo/phagolysosome and are further trimmed by proteosome. Subsequently, digested peptides are transported into the ER by TAP. MHC I molecules are produced in the ER; however, peptide loading on MHC I does not necessarily happen in the ER. Relevant evidence for this pathway includes sensitivity to proteasome inhibitors (77) and the recruitment of TAP and MHC I/peptide complex in phagosomes and endosomes (78,79).

Antigen presentation occurs in different ways in different MHC molecules. MHC I presents peptides derived primarily from cytosolic proteins while MHC II present longer antigenic peptides from the endocytic pathway (80). For the possibility of proteolytic degradation by the ubiquitin-proteasome system (UPS) in the cytosol and endolysosomal proteases, ROPs are designed to have a length of 30 amino acids between two cathepsin S cleavage sites (LRMK), so that the length of resultant peptide fragments can accommodate to both MHC I and MHC II molecules.

ROP-based vaccines compared to other cancer vaccines

Peptide-based vaccines are designed to represent full or portions of a tumour-associated antigen for vaccination. In cancer immunotherapy, peptide-based vaccines are generally safe, well-tolerated and inexpensive to manufacture. By designing a pool of overlapping peptides instead of a single-epitope peptide, this design can theoretically overcome MHC restriction and has demonstrated promising pre-clinical efficacy and certain clinical efficacy as the overlapping regions allow the possibilities for epitope diversity (81,82). ROPs as produced recombinantly as a single-chain polypeptide may be advantageous for manufacturing and drug approval compared to synthetic peptide pools (82). ROP-survivin

has been shown to stimulate both CD8+ and CD4+ T cell immune responses in *in vivo* marine studies with the potential to overcome HLA allotype restrictions (81). Not only does it provide a broader immunogenic effect compared to single epitope peptide vaccines, but also prevents off-target responses compared to vector-based vaccines.

Other potential cancer vaccines include DNA/RNA, vector-based and mRNA vaccines, etc. DNA/RNA vaccines are also inexpensive to produce with the advantage of not constricting to HLA subtypes, but they are unstable and can be rapidly eliminated (83,84). ACTs such as CAR-T cell therapy have proved clinically effective to prolong overall survival especially in haematological cancers but they are personalised and very expensive. mRNA vaccines, particularly after the COVID-19 pandemic, was found to have great potential for cancer immunotherapy. It is inexpensive, safe, well tolerated, and allows scalable production (85). Moreover, it can efficiently express multiple tumour antigens in antigen-presenting cells to facilitate both humoral and cellular adaptive immune response (85). The concept of ROP-based vaccines is the overlapping sequences linked by cathepsin S substrate sequence (LRMK). ROP sequences can be converted *in silico* into mRNA sequences and become mRNA-ROP vaccines; they can also be inserted into a vector to become vector-ROP vaccines.

Aim of this research project

We hypothesized that ROP-PSA, a recombinant artificial protein representing overlapping sequences of PSA, can be successfully and economically expressed by *E. coli* system, purified and cleaved efficiently by cathepsin S at LRMK sites, as well as trigger cytokine and chemokine release upon uptake by dendritic cells.

This project aims to develop and optimise the process of ROP-PSA expression and purification, and subsequently study the mechanism of activation of DCs *in vitro* using dendritic cell line DC2.4 by cytokine array assay. Cathepsin S digestion assay will be conducted to test if ROP-PSA can be efficiently cleaved to overlapping peptide sequences in the dendritic cells. This work is important for further vaccine development e.g. *in vivo* studies, and inform the production and optimisation of other clinically relevant ROPs.

Methods

Transformation

Both BL21 and DH5α cells are used in plasmid transformation. BL21 as protease deficient genetically engineered competent *E. coli* cells are used primarily for protein expression while DH5α, also genetically engineered competent *E. coli* cells, possess a recA1 mutation and are mainly for plasmid transformation. As the plasmids for OVM-300 were delivered internationally on filter paper, DH5α were also used to produce purer plasmids.

A. ROP-CTL-PSA

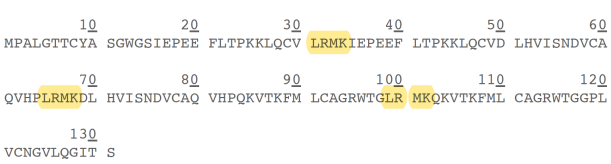

B. OVM300

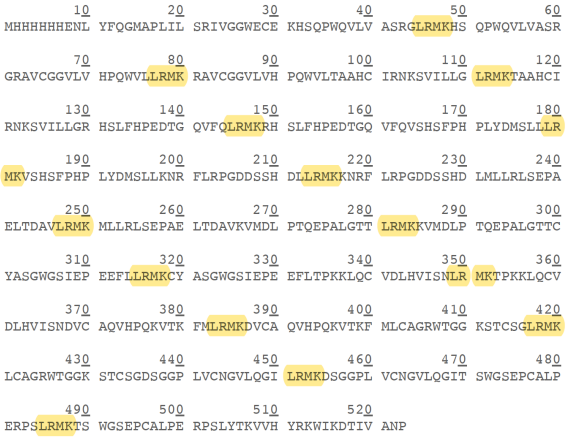

C.

	ROP-CTL-PSA		OVM300	
Molecular weight	14613.38		58821.05	
Theoretical pI	8.99		9.52	
Amino acid number	131		523	
Composition	Ala (A) 6 4.6% Arg (R) 5 3.8% Asn (N) 3 2.3% Asp (D) 4 3.1% Cys (C) 8 6.1% Gln (Q) 7 5.3% Glu (E) 6 4.6% Gly (G) 10 7.6% His (H) 4 3.1% Ile (I) 5 3.8%	Leu (L) 14 10.7% Lys (K) 11 8.4% Met (M) 6 4.6% Phe (F) 4 3.1% Pro (P) 8 6.1% Ser (S) 5 3.8% Thr (T) 9 6.9% Trp (W) 3 2.3% Tyr (Y) 1 0.8% Val (V) 12 9.2% Pyl (O) 0 0.0% Sec (U) 0 0.0%	Cys (C) 19 3.6% Ala (A) 24 4.6% Arg (R) 34 6.5% Asn (N) 10 1.9% Asp (D) 21 4.0% Gln (Q) 21 4.0% Glu (E) 21 4.0% Gly (G) 39 7.5% His (H) 27 5.2% Ile (I) 14 2.7%	Leu (L) 66 12.6% Lys (K) 34 6.5% Met (M) 24 4.6% Phe (F) 13 2.5% Pro (P) 34 6.5% Ser (S) 39 7.5% Thr (T) 24 4.6% Trp (W) 12 2.3% Tyr (Y) 7 1.3% Val (V) 40 7.6%

D.

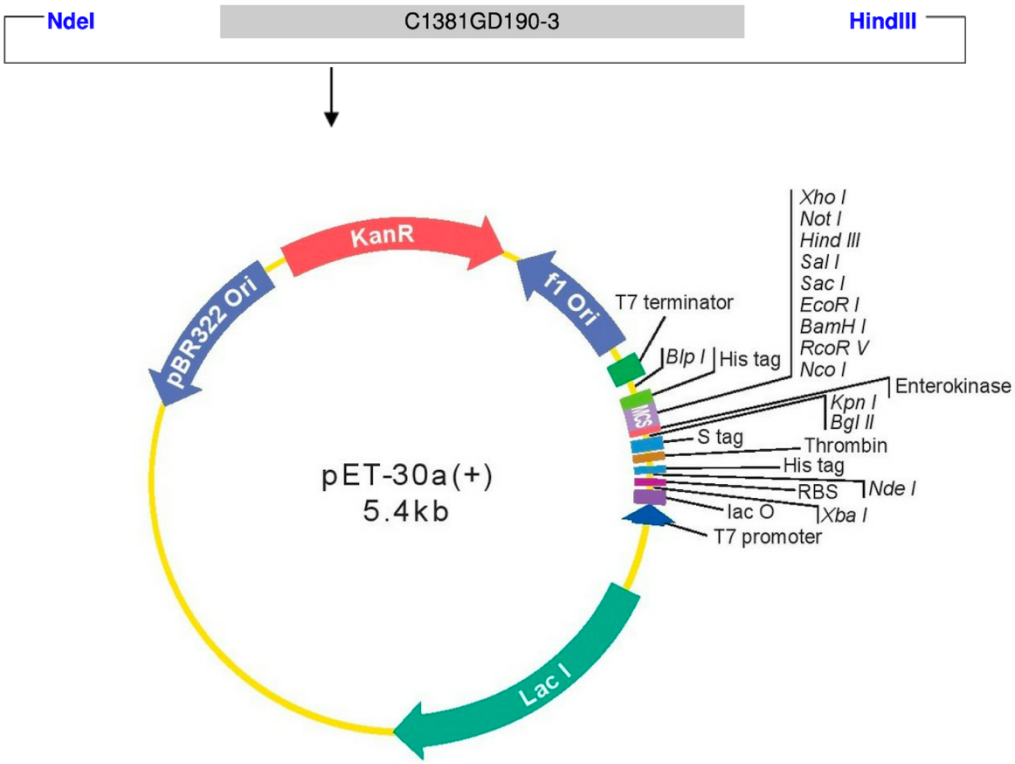

Figure 4 | Main characteristics of ROP-CTL-PSA and OVM300. (A) The amino acid sequence for ROP-CTL-PSA. **(B)** The amino acid sequence for OVM300. **(C)** Comparing main characteristics between ROP-CTL-PSA and OVM300. **(D)** The plasmid map for OVM300.

The plasmid used in this assay was cloned into pET-30a vector (Figure 4D), designed by Oxford Vacmedix, sent and shipped from Changzhou Niujin Shisong Biotechnology Company Ltd. (CNSB). The part of the filter paper which contained the plasmid was cut out within the pencil line and was folded and put into a 500 µL Eppendorf tube with a needle hole at the bottom which was placed inside a 1 mL Eppendorf tube to collect plasmid-soaked buffer. 50 µL of Tris-EDTA buffer was added to soak the paper which was then incubated for 10 minutes and centrifuged at 20000g for 1 minute to collect plasmid in solution. A tube of DH5α competent *E. coli* cells and a tube of BL-21 competent *E. coli* cells were thawed on ice until the last ice crystals disappear without vortex and mixed gently. The concentration of the plasmid was measured on Nanodrop, and 1-5 µL (1 pg - 100 ng) of plasmid DNA was added to the cells. The tube was carefully flicked 4 – 5 times to mix cells and DNA without vortexing. After 30 minutes of incubation on ice, BL21 and DH5α were heat shocked for 10 seconds and 30 seconds respectively before another placement on ice for 5 minutes. The

cell mixtures were then incubated with 950 µL of SOC medium at 37°C, 250 rpm for 60 minutes.

As the plasmid is kanamycin resistant, LB agar was made with the addition 50 µg/mL kanamycin, which was then used to make selection plates. Table 1 has demonstrated the volume of each cell mixture spread onto their respective selection plate. The plates were then incubated overnight at 37°C.

Table 1 | Distribution of cell samples onto selection plates.

Plate 1	Plate 2	Plate 3	Plate 4	Plate 5
50µL BL21 with positive control	50µL BL21 with plasmid	200µL BL21 with plasmid	50µL DH5 α with plasmid	200µL DH5 α with plasmid

Plasmid extraction

The method was used to increase plasmid purity for protein purification. The GeneJET Plasmid Maxi Prep Kit was used in this case. A single transformed DH5 α colony was transferred by a pipette tip to 250 mL LB and cultured to an OD_{600} of 2-3. The cells were harvested by centrifugation for 10 minutes at 5000 x g and the supernatant was discarded. The pelleted cells were resuspended in 6 mL of Resuspension Solution containing RNase A Solution. 6 mL of Lysis Solution was added and mixed gently by inverting the tube 4-6 times until the solution becomes viscous and slightly clear. The mixture was incubated at room temperature for 3 minutes only. Neutralization Solution (6 mL) was added and mixed immediately by inverting the tube 5-8 times. 0.8mL of the Endotoxin Binding Reagent was added and mixed immediately by inverting the tube 5-8 times and the mixture was incubated for 5 minutes at room temperature. It was noted that the neutralized bacterial lysate appeared cloudy and contained white precipitate. 6 mL of 96% ethanol was added and mixed immediately by inverting the tube 5-6 times. The mixture was centrifuged for 40 minutes at 5000 x g to pellet cell debris and chromosomal DNA. The supernatant was

transferred to a 50mL tube without disturbing the white precipitate. 6 mL of 96% ethanol was added into the supernatant and mixed immediately by inverting the tube 5-6 times.

Part of the sample (~20 mL) was transferred to the column, centrifuged for 3 minutes at 2000 x g and the flow through was discarded. This process was repeated to process remaining lysate through the purification column. Wash solution I in isopropanol (8 mL) was added to the purification column which was centrifuged for 2 minutes at 3000 x g. The flow-through was discarded. The column wash was repeated with Wash solution II in ethanol twice. The column was centrifuged for 5 minutes at 3000 x g to remove residual Wash solution and transferred to a fresh 50 mL collection tube. 1 mL of Elution Buffer was added to the centre of the purification column membrane and the column was incubated for 2 minutes at room temperature and centrifuged for 5 minutes at 3000 x g to elute plasmid DNA. The purification column was discarded. The purified plasmid DNA was used for bacterial transformation.

Protein purification for ROP-PSA

Fermentation and protein expression

A single transformed BL21 colony was picked into 100 mL LB (50 µg/mL Kan) and cultured overnight at 37°C, 250 rpm. The overnight culture was then diluted 20 times with fresh, autoclaved LB to make up 2 L and cultured until the OD600 reached 0.8. Then IPTG (final concentration of 0.5 mM) was added to induce protein expression and incubation continued at 37°C for 4 hours. The cells were harvested by centrifugation at 5000 x g for 20 minutes, weighed and frozen at -20°C before sonication.

Bacteria treatment

Once completely frozen, the harvested cells were resuspended in water at a ratio of 1:30 (net weight of cells: volume of water), and mixed by pipetting. The cell mixture was then centrifuged at 5000 x g for 30 minutes. A pellet was obtained after two washings.

Ultrasonic disruption of bacteria

The cells (pellet) were resuspended in sonification buffer (20 mM Tris-HCl pH 8.0, 1% Triton-100, 2 M Urea) at a ratio of 1:30 with addition of one tablet of protease inhibitor. Ultrasonic output power was set to 30%, 10 seconds on and 10 seconds off for 60 cycles.

Inclusion body washing

After ultrasonic treatment, the suspension was centrifuged at 20000 x g for 20 minutes. The inclusion body (pellet) was then weighed and resuspended with inclusion body washing buffer (20 mM Tris-HCl pH 8.0, 2 M urea) at a ratio of 1:30, then centrifuged at 20000 x g for 20 minutes. The washing was repeated twice, and the inclusion bodies (pellet) were weighed for later use.

Denaturation

The inclusion bodies were resuspended with denaturation solution (20 mM pH 8.0 Tris-HCl, 8 M urea, 0.3 M NaCl, 2 mM dithiothreitol (DTT), 20 mM imidazole) at a ratio of 1:25 until the mixture became homogeneous. The mixture was then stirred slowly at 4°C overnight for denaturation. The denatured inclusion bodies solution was centrifuged at 20000 x g for 30 minutes and the supernatant was obtained for nickel column chromatography.

Nickel column chromatography

A Ni-NTA resin column was prepared according to the concentration of protein (1 mL of resin can elute 20 mg protein as per product characteristics).

Batch spin method

The nickel resins were pipetted into a reaction tube (usually a 50 mL conical tube would be sufficient) and centrifuged at 500 x g for 5 minutes. The storage buffer on top was removed by careful pipetting. The resins were washed with pure water for 20 column bed volumes and centrifuged at 500 x g for 5 minutes. Water on top was removed by careful pipetting. To equilibrate the nickel resins, they were mixed with 20 column bed volumes of solution A (20 mM imidazole, 0.3 M NaCl, 2 mM DTT, 8 M urea, 20 mM Tris-HCl pH 8.0) and centrifuged at 500 x g for 5 minutes. Excess solution on top was removed. The equilibration process is recommended to repeat once. The denatured protein supernatant was added to the reaction tube and incubated for one hour at 4°C, centrifuged at 500 x g for 5 minutes afterwards and excess protein lysate removed. 5 column volumes of solution A were added to wash the resins. Washing includes mixing the solution with resins, incubating at 4°C for 10 minutes, centrifuging at 500 x g for 5 minutes and removing excess buffer. This ought to be implemented four times. The resins were then mixed with 5 mL of 5% solution B in solution A (34 mM imidazole, 0.3 M NaCl, 2 mM DTT, 8 M urea, 20 mM Tris-HCl pH 8.0) to elute out impurities. The mixture was incubated at 4°C for 10 minutes, centrifuged at 500 x g for 5 minutes and excess buffer removed. Subsequently, 5 mL of 60% solution B in solution A (188 mM imidazole, 0.3 M NaCl, 2 mM DTT, 8 M urea, 20 mM Tris-HCl pH 8.0) was mixed with resins to elute out ROP-PSA. The supernatant was obtained. Finally, 5 mL of 100% solution B (300 mM imidazole, 0.3 M NaCl, 2 mM DTT, 8 M urea, 20 mM Tris-HCl pH 8.0)was mixed with resins with the aim to wash out other unwanted impurities. The supernatant was obtained for further analysis on SDS-PAGE and western blot.

Gravity flow method

The nickel resins were pipetted into a column with a filter paper at the bottom. It is important to keep the nickel resins wet. After storage buffer flew through, the column was washed with 20 column volumes of ddH_2O. Nickel resins were equilibrated with 20 column bed volumes of solution A. A portion of less than 35 mL of samples was loaded to the column. After washing with 15 column bed volumes of solution A and 5 column bed volumes of 5% solution B, 5 mL of elution buffer (60% solution) was applied and the eluate was collected. The column was then washed with 100% solution B to elute impurities. This process was repeated for the remaining sample (less than 35 mL).

Washing Mechanism

To preserve the continuous use of the nickel column, it was washed with five column volumes of 20 mM Tris-HCL pH 8.0, 300 mM imidazole (without reducing agents), 20 column bed volumes of pure water, 10 column volumes of 20% ethanol and stored in 20% ethanol at 4 degrees.

Refolding

As ROP-PSA was solubilised and unfolded due to denaturation, refolding was conducted for the protein to return to the correct conformation and reach a biologically active form.

After optimisation, the following refolding solutions were used for step-by-step dialysis:

	Solubilisation buffer	Denaturant	Redox system	Detergent
Refolding solution 1	20 mM Tris-HCl, 300 mM NaCl	4 M urea	1 mM GSH/0.1 mM GSSG	
Refolding solution 2	20 mM Tris-HCl, 300 mM NaCl, 400 mM arginine	2 M urea	1 mM GSH/0.1 mM GSSG	0.5% sarkosyl
Refolding solution 3	20 mM Tris-HCl, 300 mM NaCl, 400 mM arginine	1M urea	1 mM GSH/0.1 mM GSSG	0.5% sarkosyl

Refolding solution 4	20 mM Tris-HCl, 300 mM NaCl, 200 mM arginine		1 mM GSH/0.1 mM GSSG	0.25% sarkosyl
Refolding solution 5	20 mM Tris-HCl, 300 mM NaCl, 200 mM arginine		1 mM GSH/0.1 mM GSSG	0.1% sarkosyl
Refolding solution 6	20 mM Tris-HCl, 300 mM NaCl, 200 mM arginine			

The pH for all refolding solutions was adjusted to between 7.2 and 7.6 for subsequent DC2.4 cell assays.

Before dialysis, all refolding solutions were prepared so that their volume was controlled 40 times of that of the collected target protein. The sample was placed in the SnakeSkin™ dialysis bag and dialysed for over 4 hours in each refolding solution at 4 degrees. It is suggested to undergo dialysis in refolding solution 1 overnight for the stabilisation of protein structure. The sample was taken for SDS-PAGE to check purity after renaturation. Then the liquid was placed at 4°C for one to two days to make sure there was no visible precipitation caused by aggregation. The sample was stored at -20°C for future use. However, repeated freeze-thaw process should be avoided in case of protein degradation.

Endotoxin Removal

Thermo Scientific Pierce High Capacity Endotoxin Removal Resin (86) was used to remove up to 99% of endotoxin and recovery is no less than 85% according to manufacturer. The spin column was centrifuged at 500 x g for one minute to remove the storage buffer. The column was washed with 0.2 N endotoxin-free NaOH overnight, followed by 2 M endotoxin-free NaCl and water for one minute each. The sample was spun down and concentrated to 1-2 mL. After equilibration with endotoxin-free phosphate-buffered saline for three times, the column was pipetted with sample and incubated at 4°C with gentle end-over-end mixing for 1 hour. The column was centrifuged at 500 x g for 1 minute to collect the sample. Endotoxin

level was measured using the Thermo Scientific Pierce LAL Chromogenic Endotoxin Quantitation Kit.

SDS-PAGE

One 4-20% 10 well comb, 50 μL/well gel (Mini Protein TGX stain free, Biorad #456-8096) was obtained from 4°C cold room. 10x running buffer was prepared by dissolving 30.0 g of Tris base, 144.0 g of glycine, and 10.0 g of SDS in 1000 ml of H_2O. The pH of the buffer should be 8.3 and no pH adjustment is required. 1x running buffer was prepared fresh before running the SDS-PAGE gel. The gel holder was assembled so that the well side of the cassette faced inwards while noting anode and cathode. The running buffer was poured into the gel box, making sure there was no leak. The gel holder was placed into the electrophoresis box and the tank was filled with running buffer up to 2 gel mark in the tank.

The samples were prepared with the addition of loading buffer to desired concentration and boiled to 95°C for 7 minutes and cooled down to 4°C. The protein marker (PageRuler Plus prestained protein ladder) was thawed. 7 µL of the marker and samples of same volume were loaded into the wells using P20 Gilson pipette slowly. The lid for the electrophoresis box was placed to match the terminal colours and plugged into the power pack. Running time and constant voltage were set up until the bottom rainbow marker reached almost the end of the cassette. For the first 15 minutes the voltage was set to 80 V and for the remaining 45 minutes it was set to 120 V. After running, the gel cassette was removed from the gel box and was opened by inserting the edge of the comb in the slot opposite the sample wells and twisting. The top plate was removed from the gel cassette.

For coomassie blue protein staining, the unwanted sides of the gel were trimmed. The cut gel was incubated in InstantBlue™ Ultrafast solution for 15 minutes at room temperature on

a shaker. It was washed in ddH_2O for 5 minutes three times on a shaker at room temperature and then left in ddH_2O with shaking overnight. The gel was placed on Biorad ChemiDoc imaging reader with the setting coomassie blue. The file was saved for later analysis.

Western blot

Transfer

A Trans-Blot Turbo (Biorad), mini format 0.2µM Nitrocellulose single application (#1704158) kit was obtained from 4°C storage. The kit stack was set up on transfer cassette, with membrane, gel and filter paper and made sure that there were no air bubbles between layers using the roller. The cassette was closed with locks secured on the sides. The program for transfer was set to 1.3 A, 25 V and run for 7 minutes. The gel was discarded. The membrane was cut to desirable size.

Ponceau staining

The membrane was placed in Ponceau stain on a shaker for 5 minutes. While the stain was discarded, the membrane was washed in ddH_2O for 5 minutes. The membrane was observed and recorded for protein presence. It was then washed with PBS for 2 minutes twice on shaker.

Blocking

The membrane was incubated in sufficient 5% skimmed milk in PBS-Tris to completely cover the membrane for 1 hour at room temperature on shaker.

Primary antibody incubation

The primary antibody was prepared by adding HRP Anti-polyHistidine antibody into 5% skimmed milk in PBS-Tris at 1:2000 to make up a total volume of 5 - 7.5 mL. The membrane was removed from the blocking solution, placed in a 50 mL Falcon tube and incubated with primary antibody solution on roller at 4°C overnight.

Development

The membrane was removed from primary antibody incubation and washed in PBS-Tris for 5 minutes three times on a shaker at room temperature. From the SuperSignalTM West Dura Extended Duration Substrate (LOT UC279798) kit, equal volume of stable Peroxide buffer and Enhance solution was mixed. The membrane was placed on a flat surface and approximately 300 µL of development solution was pipetted evenly onto the membrane. For highly expressed protein, typically less than 20 seconds of development time was enough. However for protein of low concentration, development time can be up to 10 minutes. The membrane was placed in a plastic sleeve and excessive liquid was excluded using roller and tissue paper.

Imaging

The membrane was placed on Biorad ChemiDoc imaging reader with multi-channel chemiluminescence setting for band reading and colorimetric for ladder reading. The exposure time was set to 2 minutes with an image taken every 5 seconds. The two readings were then combined to generate a western blot image.

BCA assay

Albumin standard samples were prepared with Pierce^{TM} BCA Protein Assay kit (87) and diluted with buffer (20 mM Tris-HCl, 300 mM NaCl, 200 mM arginine pH 7.4) to concentration

of 2000, 1500, 1000, 750, 500, 250, 125, 25 and 0 µg/mL. The ROP-PSA samples were prepared and diluted if needed. 25 µL of standards and samples were pipetted into a 96-well plate in which 200 µL of working reagent was added to each well. The plate was incubated at 37°C for 30 minutes and cooled to room temperature before measuring the absorbance at 562 nm on a plate reader.

To generate a standard curve, first of all the average 562 nm absorbance measurement of the blank standard replicates was subtracted from the 562 nm measurements of all other individual standard and unknown sample replicates. Therefore the standard curve was prepared by plotting the average blank-corrected 562 nm measurement for each BSA standard vs. its concentration in µg/mL. The concentrations for the unknown samples were calculated using the formula of the standard curve.

DC2.4 cell subculture

DC2.4 cells were originally obtained from K. Rock (University of Massachusetts, Worcester, Mass.) and were maintained in DC2.4 Expansion Medium which contained RPMI-1640 (Sigma Cat. No. R0883), 10% FBS (Cat. No. ES-009-B), 1x L-Glutamine (Cat. No. TMS-002-C), 1x non-essential amino acids (Cat. No. TMS-001-C), 1x HEPES Buffer Solution (Cat. No. TMS-003-C) and 0.0054x β-mercaptoethanol (Cat. No. ES-007-E).

When DC2.4 cells were approximately 80%-85% confluent, the medium was carefully removed from the T75 tissue culture flask containing the confluent layer of DC2.4 cells. Cells were washed with sterile 10 mL PBS twice which was aspirated after each rinse. 2mL trypsin was added to the flask which was incubated at 37°C for 5 minutes. This process could remove the cells from the culture flask. The flask was inspected under microscope. To ensure the complete detachment of cells, the side of the flask was gently tapped with the

palm of my hand. 8mL of media was added and mixed to neutralise trypsin. The flask was gently rotated to mix the cell suspension which was transferred to a 50 mL conical tube. The tube was centrifuged at 300 x g for 5 minutes to pellet the cells. The supernatant was discarded and the cell pellet was loosened by tapping the tip of the tube with a finger. 10 mL of DC2.4 Expansion Medium was applied to the conical tube to resuspend the cells thoroughly.

The number of cells was counted using a haemocytometer by adding 10 µL of cells with 20 µL of Trypan Blue. 10 µL of the mixed solution was loaded onto the haemocytometer and counting was conducted on at least two 4x4 grids. Cell concentration (/mL) was calculated using the following formula:

$$Cell\ concentration\left(number/_{mL}\right) = \frac{cell\ count}{number\ of\ quadrants} \times dilution\ factor \times 10000$$

According to the calculation, the cells were plated to the desired density with split ration of 1:10 to 1:15.

Cell viability MTS assay

This assay was conducted to measure the biocompatibility of the solubilising buffer and ingredients used in protein purification. For 96-well plate, 40,000 cells were needed per well which was 3.84 x 10^6 with 20% surplus for pipetting error. Therefore 4.8 x 10^6 cells were aliquoted into a 50mL conical tube which was centrifuged at 300 x g for 5 minutes. The cells were resuspended in 12 mL of medium. Medium was prepared with 1:100 Pen-strep to avoid contamination caused by buffers. 100 µL cell suspension was carefully aliquoted with multichannel pipette into a flat-bottomed 96-well plate which was incubated at 37°C for at least 4 hours for the cells to settle. The medium was removed after settlement.

500 mM Tris-HCl, 500 mM arginine, 1 M NaCl, 2 mM DTT, 8 M urea, 10% sarkosyl and the solubilising buffer (20 mM Tris-HCl, 200 mM arginine and 300 mM NaCl) were prepared. Six 1 in 2 serial dilutions with medium were made for each solution and 100 µL of which was aliquoted to its corresponding well using multichannel pipette. A triplicate for both positive control (cells + medium) and negative control (only medium) was prepared. The 96-well plate was incubated at 37°C overnight. The solution in each well was then removed and 100 µL of PBS was added instead. 10 µL of MTT labelling reagent was added to each well. The plate was incubated at 37°C for 1-4 hours – 1 hour was usually enough if there was distinct colour difference between positive and negative control. The absorbance was measured on plate reading at 570 nm wavelength. The average 562 nm absorbance measurement of the negative control replicates was subtracted from the 562 nm measurements of all other replicates.

Cytokine array

This assay was applied to investigate cytokine release from DC2.4 cells upon antigen uptake and presentation. This method was adopted from protocol provided from bio-techne Proteome Profile Mouse Cytokine Array Kit, Panel A (88).

Sample preparation

A 6-well plate was used and approximately 1.2 x 10^6 DC2.4 cells were pipetted into each well (see DC2.4 cells subculture). The cells were incubated at 37°C for at least 4 hours to settle. Subsequently all culture medium was aspirated from the wells. For well 1, 250 µL ROP-PSA in buffer (20 mM Tris-HCl, 300 mM NaCl, 200 mM arginine, pH 7.4) was added to the cells so that the concentration of ROP-PSA reached 200 µg/2 mL while in well 2, that of ROP-PSA was 40 µg/2 mL. Well 3 was used as negative control where 250 µL of buffer was added. For well 4 nothing was added apart from cell medium for baseline cytokine

measurement. For well 5, 4 µL of eBioscience™ Lipopolysaccharide (LPS) Solution 500x was added so that its concentration reached 5µg/mL, which was used to compare endotoxin-induced response with ROP-PSA. Medium was added to the wells for total volume of 2mL in each well. The plate was incubated overnight at 37°C. Cell culture supernatant was aliquoted to five Eppendorf tubes which were centrifuged at 300 x g for 5 minutes to obtain sample supernatant.

Blocking

Array buffer 6 (2mL) (as a block buffer) was pipetted into each well of the 4-well multi-dish to be used. Each membrane was removed with flat-tip tweezers from between the protective sheets and placed in a well of the 4-well multi-dish. The number on the membrane should be facing upward. Upon contact with array buffer 6, the blue dye from the spots will disappear, but the capture antibodies are retained in their specific locations. The membranes were incubated for one hour on a rocking platform shaker. The tray was oriented so that each membrane was rocked end to end in its well.

Primary antibody incubation

When the membranes were blocking, samples were prepared by adding up to 1 mL of each sample to 0.5 mL of array buffer 4 in separate tubes. In times of insufficient samples, array buffer 6 was used to adjust the final volume to 1.5 mL. 15 µL of reconstituted Mouse Cytokine Array Panel A Detection Antibody Cocktail was added to each prepared sample which was incubated at room temperature for one hour. Array Buffer 6 was aspirated from the wells of the 4-Well Multi-dish and the sample/antibody mixture was added instead. The dish was incubated overnight at 4°C on a rocking platform shaker.

Secondary antibody incubation

Each membrane was carefully removed and placed into individual plastic containers with 20 mL of 1x Wash Buffer. Each membrane was washed with 1x Wash Buffer for 10 minutes on a rocker platform shaker for three times. Streptavidin-HRP was diluted in Array Buffer 6 using the dilution factor on the label. 2.0 mL of diluted Streptavidin-HRP was pipetted into each well of the 4-Well Multi-dish. Each membrane was removed from its wash container, returned to the 4-Well Multi-dish containing the diluted Streptavidin-HRP and incubated for 30 minutes at room temperature on a rocking platform shaker. The membranes were washed three times again as described before.

Development

Each membrane was removed from its wash container. The lower edge of the membranes was blotted onto paper towels and allowed excess Wash Buffer to drain. Each membrane was placed on the bottom sheet of the plastic sheet protector with the identification number facing up. 300 µL of the prepared Chemi Reagent Mix (mixed in equal volumes of Chemi Reagent 1 and 2) was pipetted onto each membrane evenly. After optimisation, the membranes were incubated in solution for 10 minutes.

Imaging

The membranes were placed on Biorad ChemiDoc imaging reader with multi-channel chemiluminescence setting. The exposure time was set to 2 minutes with an image taken every 10 seconds.

Cathepsin S Digestion Assay

1 µL of 1 M DTT was added to 200 µL of 700 µg/mL ROP-PSA (validated by BCA assay) in an Eppendorf tube to make up 4 mM DTT. The solution was divided into two equal portions

of 100 µL. Human Cathepsin S (SinoBiological, 10487-H08H) was added to a final protease: ROP ratio of 1:50 (w/w) and 1:100 (w/w). The mixture was incubated at 37°C overnight and 12 µL of sample was removed respectively at 0-hour, 0.5-hour, 1-hour, 2-hour, 4-hour, and overnight. The extent of digestion was determined by subjecting the aliquot to SDS-PAGE. Cathepsin digestion can be stopped by storing at -20°C or boiling up to 95°C. SDS-PAGE gel and samples were sent to mass spectrometry analysis.

Results

This project started with the protocol optimisation for the expression and purification of two artificial ROPs: ROP-CTL-PSA and OVM300, especially in terms of denaturation and refolding conditions. OVM300 was then tested in cytokine array assays with murine DC2.4 cell line to investigate cytokine release. Finally cathepsin digestion assay was conducted to investigate cathepsin S cleavage on OVM300 via mass spectrometry.

Developing products: ROP-CTL-PSA and OVM300

Sequences for the two ROPs being developed are illustrated on Figure 4A and B. ROP-CTL-PSA is designed based on cytotoxic T lymphocyte epitopes and OVM300 based on both CD4+ and CD8+ T cell epitopes.

Figure 4C has listed different characteristics (molecular weight, pI, amino acid number, composition of amino acids) that affect protein aggregation during expression and purification. Both products are recombinant insoluble proteins that form inclusion bodies at expression stage, require denaturant for solubilisation and are ultimately refolded to biologically active forms. This is a time-consuming process and often requires a trial-and-error procedure. ROP-CTL-PSA has a low molecular weight while OVM300 has a high molecular weight which increases the risk of aggregation. Almost half of the amino acids of ROP-CTL-PSA and OVM300 are hydrophobic (alanine (Ala, A), valine (Val, V), leucine (Leu, L), isoleucine (Ile, I), proline (Pro, P), phenylalanine (Phe, F) and cysteine (Cys)). High molecular weight and high composition of hydrophobic residues in *E. coli* expression system increase the possibility of inclusion bodies formation which is a cytoplasmic insoluble aggregate formed during expression stage (89). On the other hand, the two products have similar theoretical pI which can affect their net charge at different pH. This could be a decisive factor on choosing the application of chromatography and buffer pH.

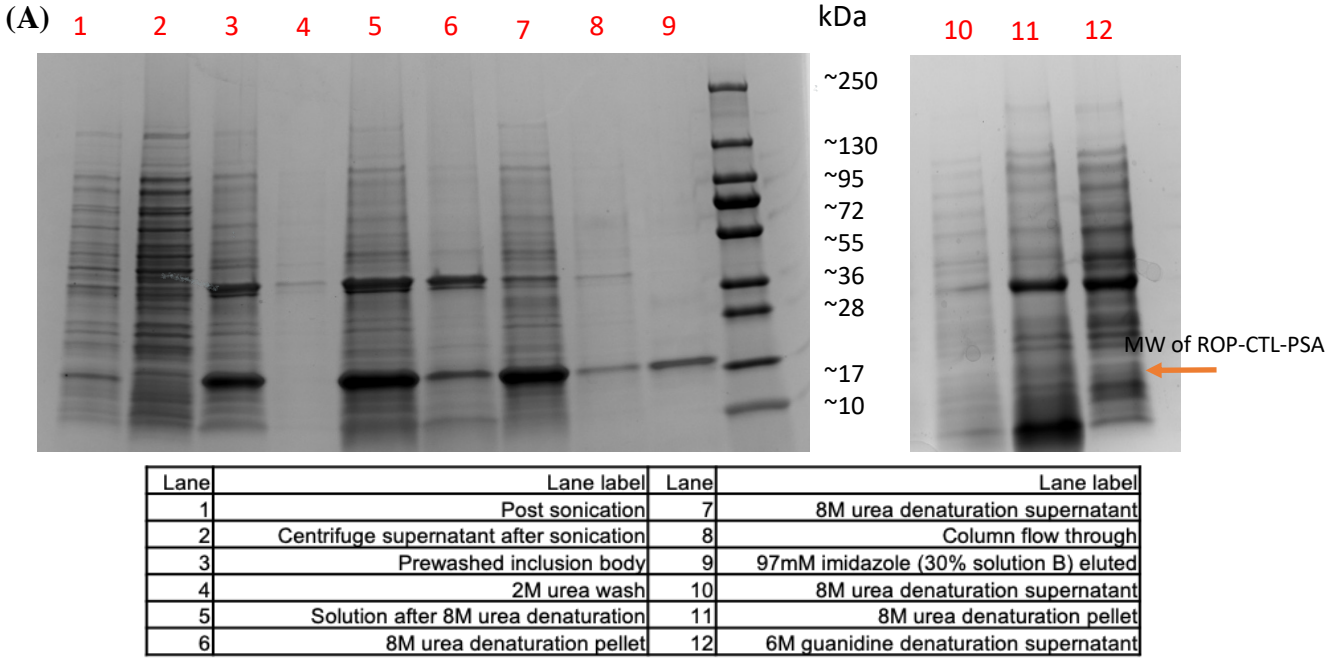

Lane	Lane label	Lane	Lane label
1	Post sonication	7	8M urea denaturation supernatant
2	Centrifuge supernatant after sonication	8	Column flow through
3	Prewashed inclusion body	9	97mM imidazole (30% solution B) eluted
4	2M urea wash	10	8M urea denaturation supernatant
5	Solution after 8M urea denaturation	11	8M urea denaturation pellet
6	8M urea denaturation pellet	12	6M guanidine denaturation supernatant

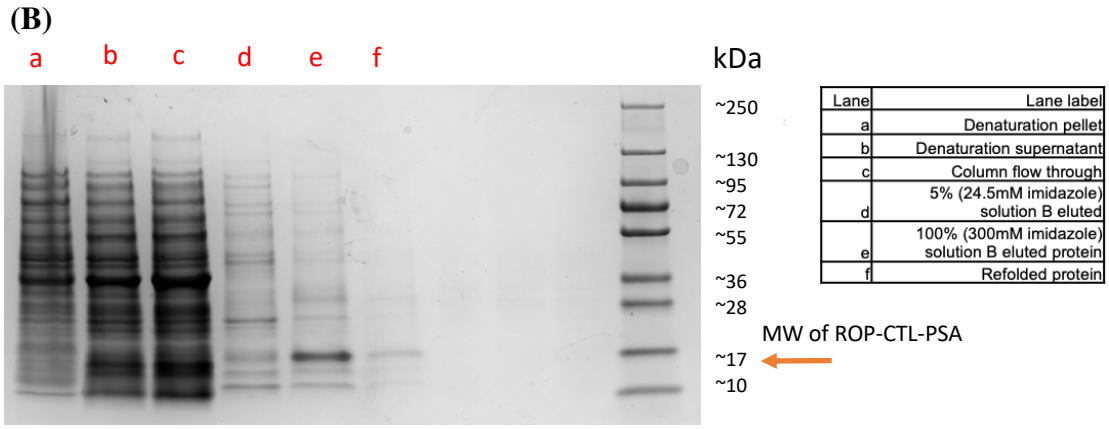

Lane	Lane label
a	Denaturation pellet
b	Denaturation supernatant
c	Column flow through
d	5% (24.5mM imidazole) solution B eluted
e	100% (300mM imidazole) solution B eluted protein
f	Refolded protein

Figure 5 | Expression and purification of ROP-PSA (Product: ROP-CTL-PSA). Process for ROP-CTL-PSA expression from *E. coli* system and solubilisation was optimised and validated by SDS-PAGE. Orange arrows indicate the bands for ROP-CTL-PSA. **(A)** Illustration of SDS-PAGE gel analysis as a result of expression and solubilisation before (lane 1-9) and after optimisation (lane 10-12). **(B)** Illustration of SDS-PAGE as a result of solubilisation and purification of ROP-CTL-PSA using nickel column chromatography. A lower concentration (10 mM) of imidazole in solution A was trialled in this case.

Product ROP-CTL-PSA was firstly expressed in *E. coli* system and purified with Ni affinity column in this project. It has a molecular weight of approximately 15 kDa, so its presence is indicated by orange arrows (Figure 5). Remarkably visible band (purity: 5.81%) on Figure 5A lane 3 i.e. inclusion bodies represents successful expression of such protein from *E. coli* expression system. With 8 M urea for denaturation, Figure 5A lanes 6 and 7 represent the pellet and the supernatant respectively; Figure 5A lane 7 visibly has a stronger band than

lane 6 and a higher purity. With 6 M guanidine, the purity of the sample (Figure 5A lane 12) remarkably decreased, and the intensity of the desired band is weaker than that of Figure 5A lane 10.

Figure 5B lane b and c being almost identical indicates weak binding of ROP-CTL-PSA to nickel column. Results from Figure 5A were not reproducible. The desired bands are weak from imidazole eluted samples (Figure 5B lane d and e) and of low purity which indicated unsuccessful purification from nickel column chromatography. Other purification methods would need to be sourced. Moreover, the design of ROP-CTL-PSA may contribute to inadequate response by both CD4+ and CD8+ T cells because of insufficient epitope coverage. Due to time limitation another product OVM300 was expressed and tested instead.

Protocol optimisation for the purification of OVM300

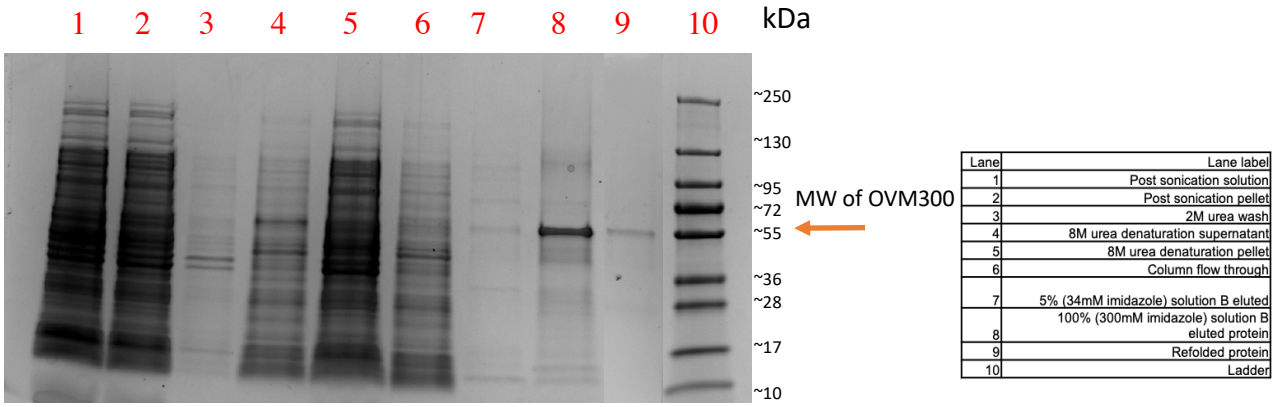

Lane	Lane label
1	Post sonication solution
2	Post sonication pellet
3	2M urea wash
4	8M urea denaturation supernatant
5	8M urea denaturation pellet
6	Column flow through
7	5% (34mM imidazole) solution B eluted
8	100% (300mM imidazole) solution B eluted protein
9	Refolded protein
10	Ladder

Figure 6 | Expression and purification of ROP-PSA (Product: OVM300) demonstrated by SDS-PAGE. Original protocol for OVM300 expression from *E. coli* system and solubilisation and purification was trialled. Before optimisation, no dithiothreitol (DTT) was used for expression and inclusion bodies wash. 8 M urea and 1 mM DTT were used for denaturation, and 10 mM imidazole (a lower concentration) was applied for in solution A. The initial refolding conditions are shown on Table 2 row A.

OVM300 has the molecular weight of approximately 59 kDa as indicated by the orange arrow. Lane 1 indicated successful expression of OVM300 from *E. coli* system. Little amount of unwanted protein was washed out by 2 M urea (lane 3). Normalised ratio of the intensity of the desired band on lane 4 (denaturation supernatant) to that on lane 5 (denaturation

pellet) is 0.55 (<1) which indicates more protein remains in the pellet than in the supernatant. The sample processed by nickel column chromatography (lane 8) has the purity of 9% and only a weak band remained in lane 9 (refolded protein) due to significant precipitation. Therefore, denaturation, nickel affinity chromatography and refolding conditions need to be further optimised.

Denaturation

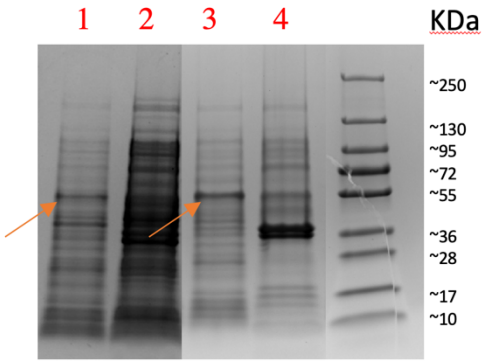

Lane	Lane label
1	1mM DTT supernatant
2	1mM DTT pellet
3	2mM DTT supernatant
4	2mM DTT pellet

Figure 7 | Illustration of SDS-PAGE gel to compare the effect of 1 mM DTT and 2 mM DTT on OVM300 solubilisation. Orange arrows represents the OVM300 bands in denaturation supernatant.

Figure 7 shows the effects of different concentration of DTT in OVM300 solubilisation. 2 mM DTT was used instead of 1 mM DTT in addition to 8 M urea in the denaturation solution. Normalised ratio of the intensity of the desired band on lane 3 to that on lane 1 is 1.89 (>1) which indicates more protein was extracted by using 2 mM DTT, 8 M urea than 1 mM DTT, 8 M urea. It was also noticeable that there is a prominent band at ~36 kDa on lane 4 that deserved further investigation. It can be the truncated version of OVM300 or just impurities. A western blot will be conducted for this (Figure 9). In short, denaturation efficiency was superior with 2 mM DTT.

Nickel chromatography

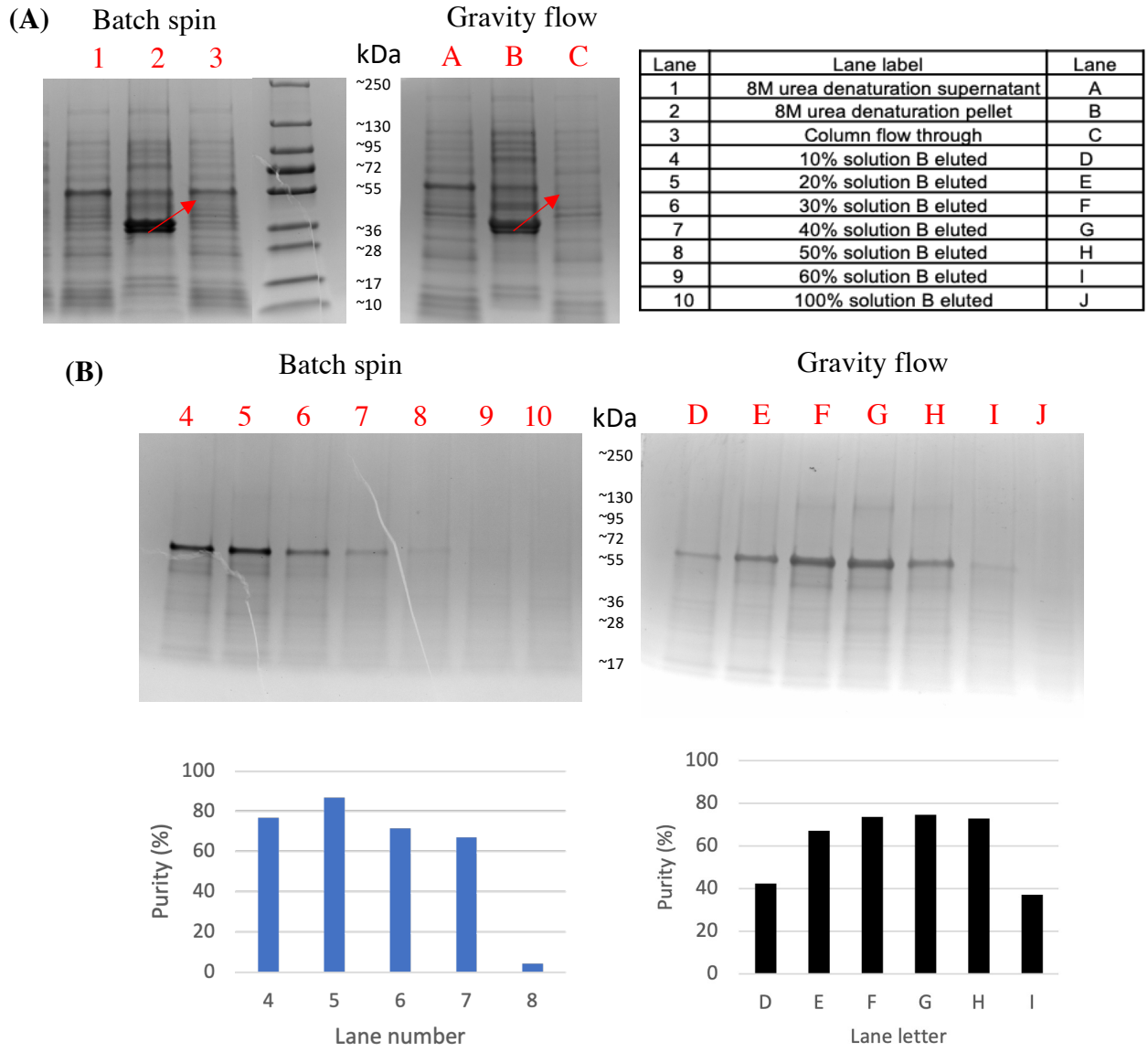

Lane	Lane label	Lane
1	8M urea denaturation supernatant	A
2	8M urea denaturation pellet	B
3	Column flow through	C
4	10% solution B eluted	D
5	20% solution B eluted	E
6	30% solution B eluted	F
7	40% solution B eluted	G
8	50% solution B eluted	H
9	60% solution B eluted	I
10	100% solution B eluted	J

Figure 8 | Comparing yield and purity between the application of batch spin and gravity flow in nickel chromatography for protocol optimisation. Illustration of SDS-PAGE gels for batch spin and gravity flow nickel column chromatography – **(A)** column flow through. **(B)** protein elution. Solution A: 20mM imidazole, 0.3M NaCl, 2mM DTT, 8M urea, 20mM Tris-HCl pH 8.0; solution B: 300mM imidazole, 0.3M NaCl, 2mM DTT, 8M urea, 20mM Tris-HCl pH 8.0.

Both batch spin and gravity flow methods were trialled in nickel chromatography for protocol optimisation (Figure 8). In batch spin (Figure 8A, lane 1-3), approximately 77% of OVM300 remained in column flow through (lane 3) whereas in gravity flow (Figure 8A, lane A-C), only 5% of OVM300 was lost in the column flow through while significant amount of impurities was washed out.

Two bar charts were graphed for protein elution for both methods and different patterns can be observed from the charts. Purity of samples from batch spin ranges from 67% to 86% apart from one outlier at 50% solution B (Figure 8B, lane 8) despite the low yield. However, gravity flow was preferred as it generally constructed a clear elution gradient where the experiment can be designed to obtain a higher purity.

Validation by western blot

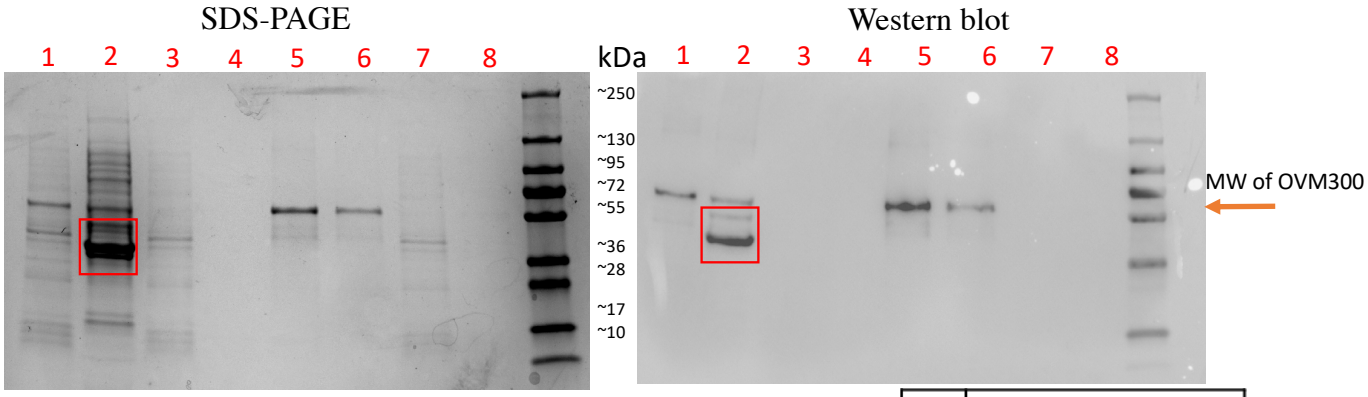

Lane	Lane label
1	Denaturation supernatant
2	Denaturation pellet
3	Column flow through
4	5% solution B eluted
5	**60% solution B eluted**
6	**100% solution B eluted**
7	Column flow through II
8	**60% solution B eluted II**

Figure 9 | Illustration of SDS-PAGE and western blot for the same samples (1-8). 5% solution B was applied to nickel affinity chromatography to wash out protein impurities. Subsequently, 60% solution B was applied to obtain OVM300; then 100% solution B was applied to wash out all proteins from the nickel column.

Figure 9 shows the illustration of SDS-PAGE and western blot of the same samples from denaturation and nickel affinity chromatography. SDS-PAGE was conducted here to investigate the purity of OVM300 during purification. Western blot was used to confirm the presence of OVM300 in the samples as the antibody used in western blot was HRP-conjugated anti-polyHistidine which binds to histidine residues at N-terminus of OVM300. There is presence of His-tag protein on lane 1, 2, 5 and 6. Lane 1 shows 47.08% purity of OVM300 in denaturation supernatant estimated by ImageLab. It is interesting to note the possible presence of truncated OVM300 as indicated by the red bracket on lane 2 in the denaturation pellet from SDS-PAGE and confirmed by western blot. However it could also be non-specific antibody binding on the western blot. The purity of the band on lane 5 was

at least 87.33%; however the purity of OVM300 might be higher given the presence of bands of lower molecular weight on the western blot. Sample from lane 3 (column flow through from 1st nickel column chromatography) was reapplied for purification but both SDS-PAGE and western blot showed no signs of OVM300 in the second 60% solution B elution (lane 8). In summary, protocol for the purification of OVM300 was successfully optimised and the project was ready to move on to solubilising the protein in biocompatible refolding solution.

Screening buffer ingredients for cell viability

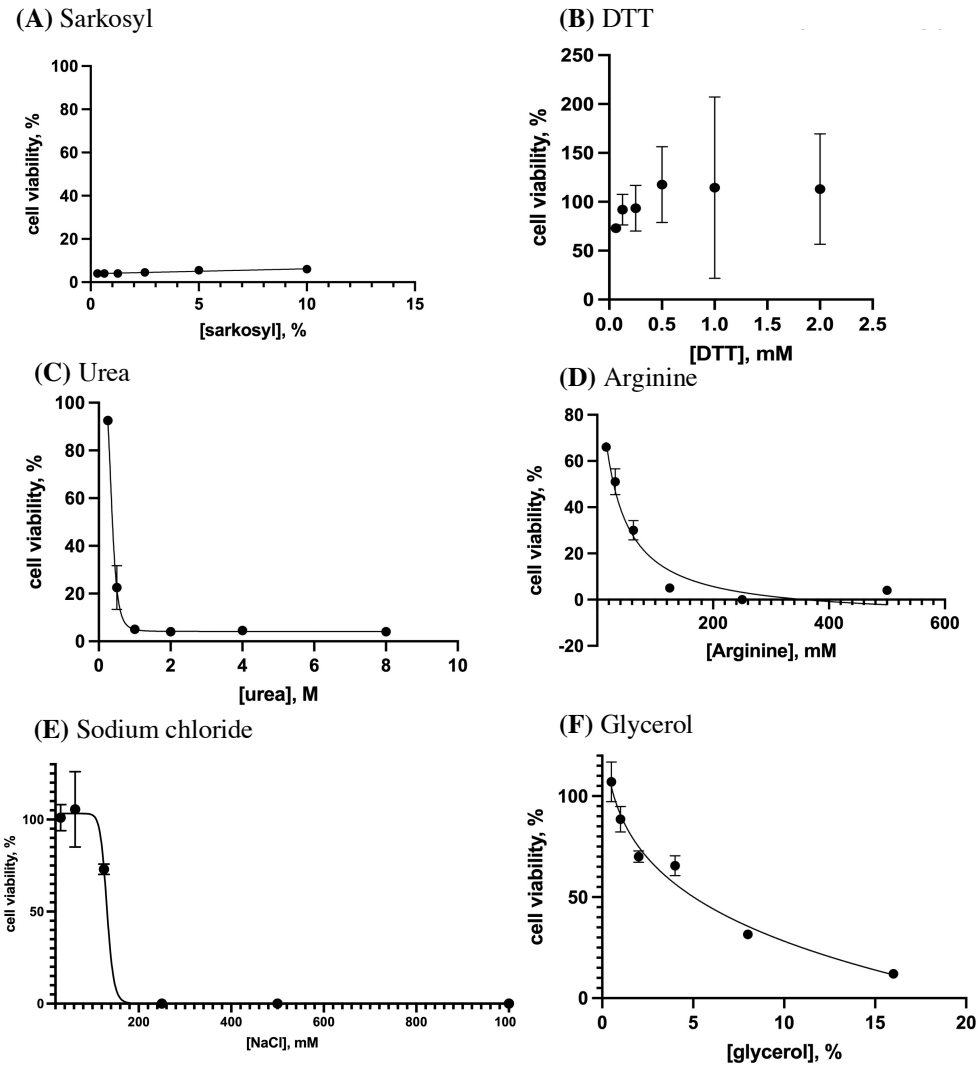

Figure 10 | Effects of individual buffer ingredients of different concentrations used in protein purification and refolding, on DC2.4 cell viability. Graphs show mean ± standard deviation of triplicate technical replicates from single experiment. **(A)** sarkosyl; **(B)** DTT; **(C)** urea; **(D)** arginine; **(E)** sodium chloride; **(F)** glycerol.

Figure 10 shows the MTS assays to evaluate the effect on cell viability of different buffer components so as to provide an idea for the recipe of the buffer used to solubilise OVM300 for subsequent DC2.4 cell assays.

Generally, DC2.4 cell viability decreased as the concentration of the ingredient increased. Sarkosyl as a detergent is highly cytotoxic as cell viability remained below 10% from 10% concentration to 0.3125%. Cell viability for DTT was between 75% and 100% even at 2 mM; however this experiment needs repetition as significant variability of cell viability was observed in triplicates. Urea had a detrimental effect on cell viability as well, dropping from 90% at 0.125 M to 20% at 0.25 M, remaining below 10% from 0.5 M. Arginine, surprisingly, seemed to affect cell viability even at the lowest concentration (12.5 mM) although the alkaline pH environment may be a prominent contributory factor to this result. Sodium chloride and glycerol were tolerable with cell viability higher than 80% at low concentration: lower than 100 mM and 2.5% respectively. The results of these experiments provided important information for refolding optimisation.

Optimising refolding

	Different refolding conditions trialled	Protein precipitation	Resultant concentration	Recovery
A	1. 4 M urea 2. 2 M urea, 0.1% sarkosyl 3. 1 M urea, 0.1% sarkosyl 4. 0 M urea	++		
B	1. 4 M urea 2. 2 M urea, 0.25% sarkosyl 3. 1 M urea, 0.25% sarkosyl 4. 0 M urea	+++		
C	1. 4 M urea, 2% Tween-80 2. 2 M urea, 0.25% sarkosyl, 2% Tween-80 3. 1 M urea, 0.1% sarkosyl, 2% Tween-80 4. 0 M urea, 2% Tween-80	+		
D	1. 4 M urea 2. 2 M urea, 0.25% sarkosyl 3. 1 M urea, 0.1% sarkosyl 4. 0 M urea	+++		
E	1. 4 M urea, 1 mM DTT 2. 2 M urea, 0.25% sarkosyl, 1 mM DTT 3. 1 M urea, 0.1% sarkosyl, 1 mM DTT 4. 0 M urea, 0.1% sarkosyl, 1 mM DTT 5. 0 M urea	+++ 2 M urea to 1 M urea	0.14 mg/mL in 2.5 mL	17.5%
F	1. 4 M urea, 1 mM DTT 2. 2 M urea, 1 mM DTT, 0.4 M arginine, 0.5% sarkosyl 3. 1 M urea, 1 mM DTT, 0.4 M arginine, 0.5% sarkosyl 4. 0 M urea, 1 mM DTT, 0.2 M arginine, 0.25% sarkosyl 5. 0 M urea, 1 mM DTT, 0.1M arginine, 0.1% sarkosyl 6. 0 M urea, 0.1 M arginine	++ (5) to (6) (overnight)	0.03 mg/mL in 4.5 mL	27%
G	1. 4 M urea, 1 mM DTT 2. 2 M urea, 1 mM DTT, 0.4 M arginine, 0.5% sarkosyl 3. 1 M urea, 1 mM DTT, 0.4 M arginine, 0.5% sarkosyl 4. 0 M urea, 1 mM DTT, 0.2 M arginine, 0.25% sarkosyl 5. 0 M urea, 1 mM DTT, 0.2 M arginine, 0.1% sarkosyl 6. 0 M urea, 0.2 M arginine	- Precipitation after two days of storage	0.27 mg/mL in 2.5 mL	100%

H	1. 4 M urea, 1 mM GSH/0.1 mMGSSG 2. 2 M urea, 1 mM GSH/0.1 mMGSSG, 0.4 M arginine, 0.5% sarkosyl 3. 1 M urea, 1 mM GSH/0.1 mMGSSG, 0.4 M arginine, 0.5% sarkosyl 4. 0 M urea, 1 mM GSH/0.1 mMGSSG, 0.2 M arginine, 0.25% sarkosyl 5. 0 M urea, 1 mM GSH/0.1 mMGSSG, 0.2 M arginine, 0.1% sarkosyl 6. 0 M urea, 0.2 M arginine	-	0.27 mg/mL in 2.5 mL	100%
I	1. 4 M urea, 1 mM GSH/0.1 mMGSSG, pH7.4 2. 2 M urea, 1 mM GSH/0.1 mMGSSG, 0.4 M arginine, 0.5% sarkosyl, pH7.4 3. 1 M urea, 1 mM GSH/0.1 mMGSSG, 0.4 M arginine, 0.5% sarkosyl, pH7.4 4. 0 M urea, 1 mM GSH/0.1 mMGSSG, 0.2 M arginine, 0.25% sarkosyl, pH 7.4 5. 0 M urea, 1 mM GSH/0.1 mMGSSG, 0.2 M arginine, 0.1% sarkosyl, pH 7.4 6. 0 M urea, 0.2 M arginine, pH 7.4	+	0.03 mg/mL in 20 mL	30%

Table 2 | Protein precipitation under different refolding conditions.

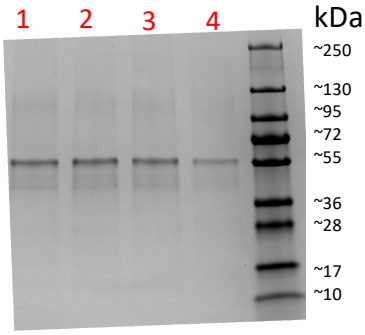

Lane	Lane label	Purity %
1	After refolding	82.47
2	After refolding	88.95
3	After spinning down	84.49
4	After endotoxin removal	82.67

Figure 11 | SDS-PAGE for refolding, protein concentration and endotoxin removal.

A variety of refolding conditions has been trialled to obtain the highest yield in the least cytotoxic buffer environment as shown on table 2. At the end (table 2I), while the concentration of urea was taken down gradually, sarkosyl and arginine were added as they had similar functions as urea. Meanwhile a redox system (GSH/GSSG) was used to facilitate a favourable environment for protein renaturation due to their abilities to oxidize thiolates and reduce incorrect disulphide bonds (90). pH was also adjusted to 7.4 for DC2.4 cell viability as arginine is alkalic. After refolding, it was necessary to spin down the sample to 1-4 mL for endotoxin removal. Although about 50% of OVM300 was lost by endotoxin

removal according to Nanodrop, purity stayed stable at around 80-90% during protein concentration and endotoxin removal process.

Investigating biocompatibility of OVM300 and solubilising buffer in MTS assays

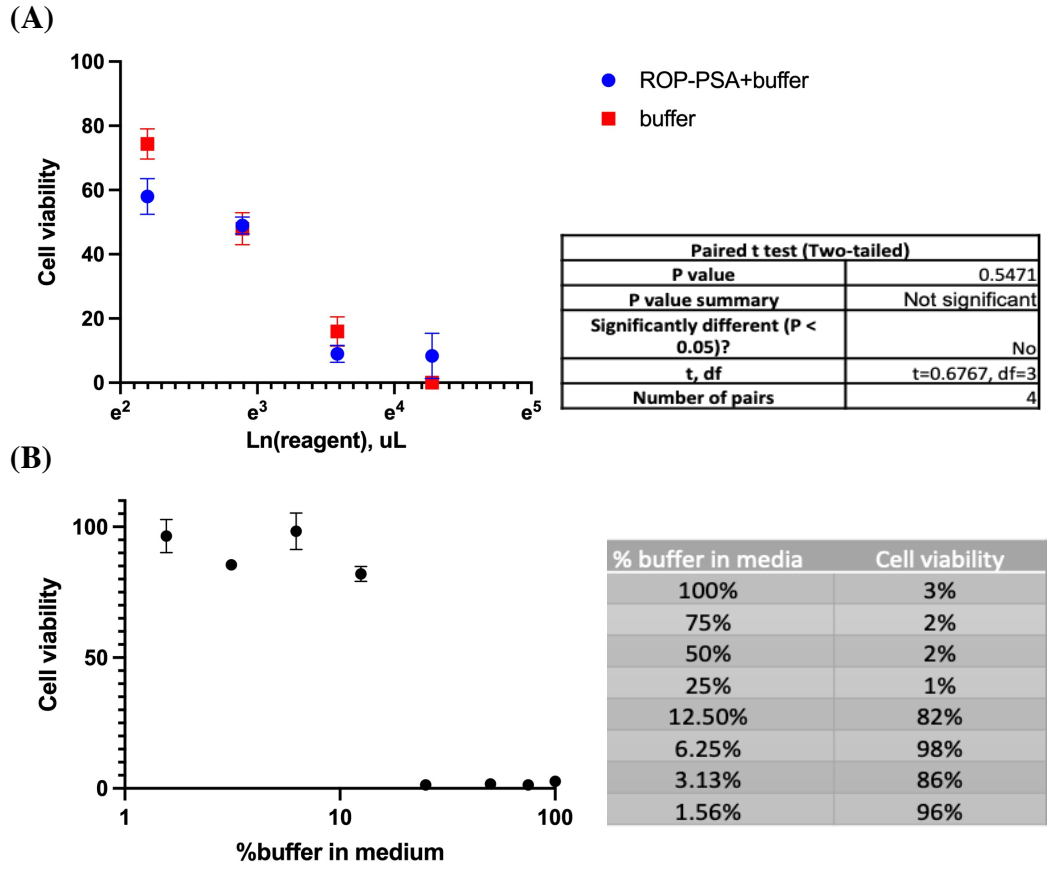

Paired t test (Two-tailed)	
P value	0.5471
P value summary	Not significant
Significantly different (P < 0.05)?	No
t, df	t=0.6767, df=3
Number of pairs	4

% buffer in media	Cell viability
100%	3%
75%	2%
50%	2%
25%	1%
12.50%	82%
6.25%	98%
3.13%	86%
1.56%	96%

Figure 12 | (A) Comparing the effects on DC2.4 cell viability between buffer (20mM Tris-HCl, 300mM NaCl, 200mM arginine, pH 7.4) and ROP-PSA (OVM300) in buffer using a paired t test ($p<0.05$, $df=3$). Graph shows mean ± standard deviation of duplicate technical replicates from single experiment. **(B)** Effects of buffer of different percentages in medium on DC2.4 cell viability. Graphs show mean ± standard deviation of duplicate technical replicates from single experiment.

A paired t test (Figure 12A) was conducted to investigate if there was a statistically significant difference in cell viability with OVM300 in buffer and buffer alone, hence deducing if OVM300 influences cell viability. Four samples of different concentration and triplicates for each sample were used for both OVM300 and buffer. According to the two-tailed paired t test, there was not an average difference in cell viability between OVM300 in buffer and buffer alone ($t_3=0.6767$, $p<0.05$). As a result, OVM300 did not affect cell viability.

MTS assay was conducted to investigate cell viability under different concentration of the solubilising buffer (20mM Tris HCl, 300mM NaCl, 200mM arginine, pH 7.4) to decide the percentage proportion of OVM300 to put in for cytokine array assays. Cell viability

maintained higher than 80% from 12.5% despite a sudden drop at 25% to below 5%. To be safe, 6.25% was selected as the optimal percentage concentration for subsequent cell assays.

Quantification for ROP-PSA concentration

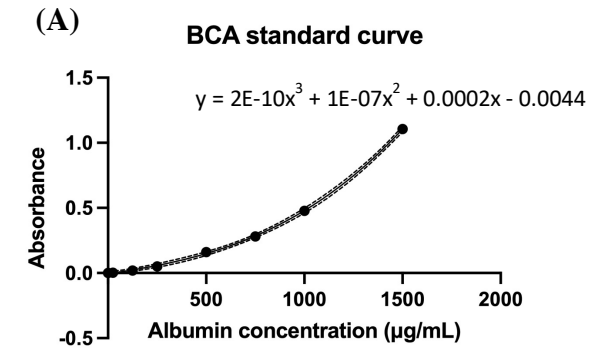

ROP-PSA Samples	Absorbance	Concentration (µg/mL)
BEFORE endotoxin removal	0.364	861.79

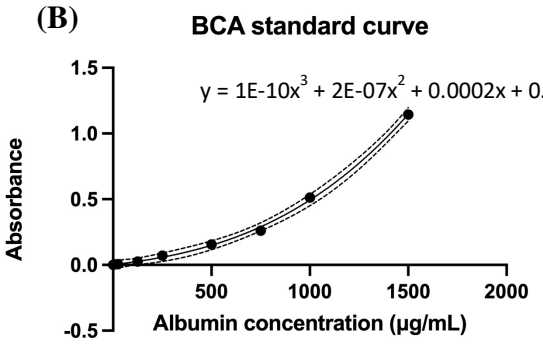

ROP-PSA Samples	Absorbance	Concentration (µg/mL)
AFTER endotoxin removal	0.325	800.095

Figure 13 | Quantification of OVM300 concentration by the application of BCA assays. (A) Quantification before endotoxin removal. **(B)** Quantification after endotoxin removal.

BCA assays were conducted (Figure 13) to estimate the concentration of this artificial protein OVM300. The solubilising buffer (20mM Tris HCl, 300mM NaCl, 200mM arginine, pH 7.4) was used to dilute the samples. The concentration of both OVM300 before endotoxin removal and after endotoxin removal was investigated. A third-order fitted standard curve was generated for both occasions. Endotoxin removal contributed to 7.16% loss in protein in this case. More than 800µg of protein were obtained from both purification processes.

Cytokine release confirmed by cytokine array assays

Coordinate	Target/Control	Alternate Nomenclature
A1, A2	Reference Spot	—
A23, A24	Reference Spot	—
B1, B2	BLC	CXCL13/BCA-1
B3, B4	C5/C5a	Complement Component 5a
B5, B6	G-CSF	—
B7, B8	GM-CSF	—
B9, B10	I-309	CCL1/TCA-3
B11, B12	Eotaxin	CCL11
B13, B14	ICAM-1	CD54
B15, B16	IFN-γ	—
B17, B18	IL-1α	IL-1F1
B19, B20	IL-1β	IL-1F2
B21, B22	IL-1ra	IL-1F3
B23, B24	IL-2	—
C1, C2	IL-3	—
C3, C4	IL-4	—
C5, C6	IL-5	—
C7, C8	IL-6	—
C9, C10	IL-7	—
C11, C12	IL-10	—
C13, C14	IL-13	—
C15, C16	IL-12 p70	—
C17, C18	IL-16	—
C19, C20	IL-17	—
C21, C22	IL-23	—
C23, C24	IL-27	—

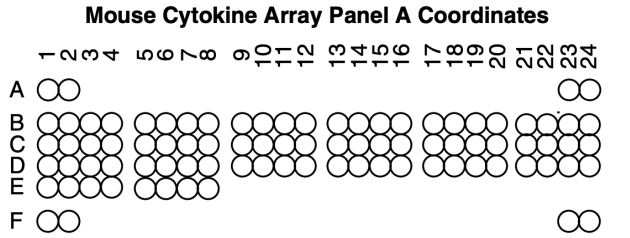

Coordinate	Target/Control	Alternate Nomenclature
D1, D2	IP-10	CXCL10/CRG-2
D3, D4	I-TAC	CXCL11
D5, D6	KC	CXCL1
D7, D8	M-CSF	—
D9, D10	JE	CCL2/MCP-1
D11, D12	MCP-5	CCL12
D13, D14	MIG	CXCL9
D15, D16	MIP-1α	CCL3
D17, D18	MIP-1β	CCL4
D19, D20	MIP-2	CXCL2
D21, D22	RANTES	CCL5
D23, D24	SDF-1	CXCL12
E1, E2	TARC	CCL17
E3, E4	TIMP-1	—
E5, E6	TNF-α	—
E7, E8	TREM-1	—
F1, F2	Reference Spot	—
F23, F24	PBS (Negative Control)	Control (-)

Figure 14 | Mouse cytokine array panel A coordinates for reference adapted from the protocol booklet.

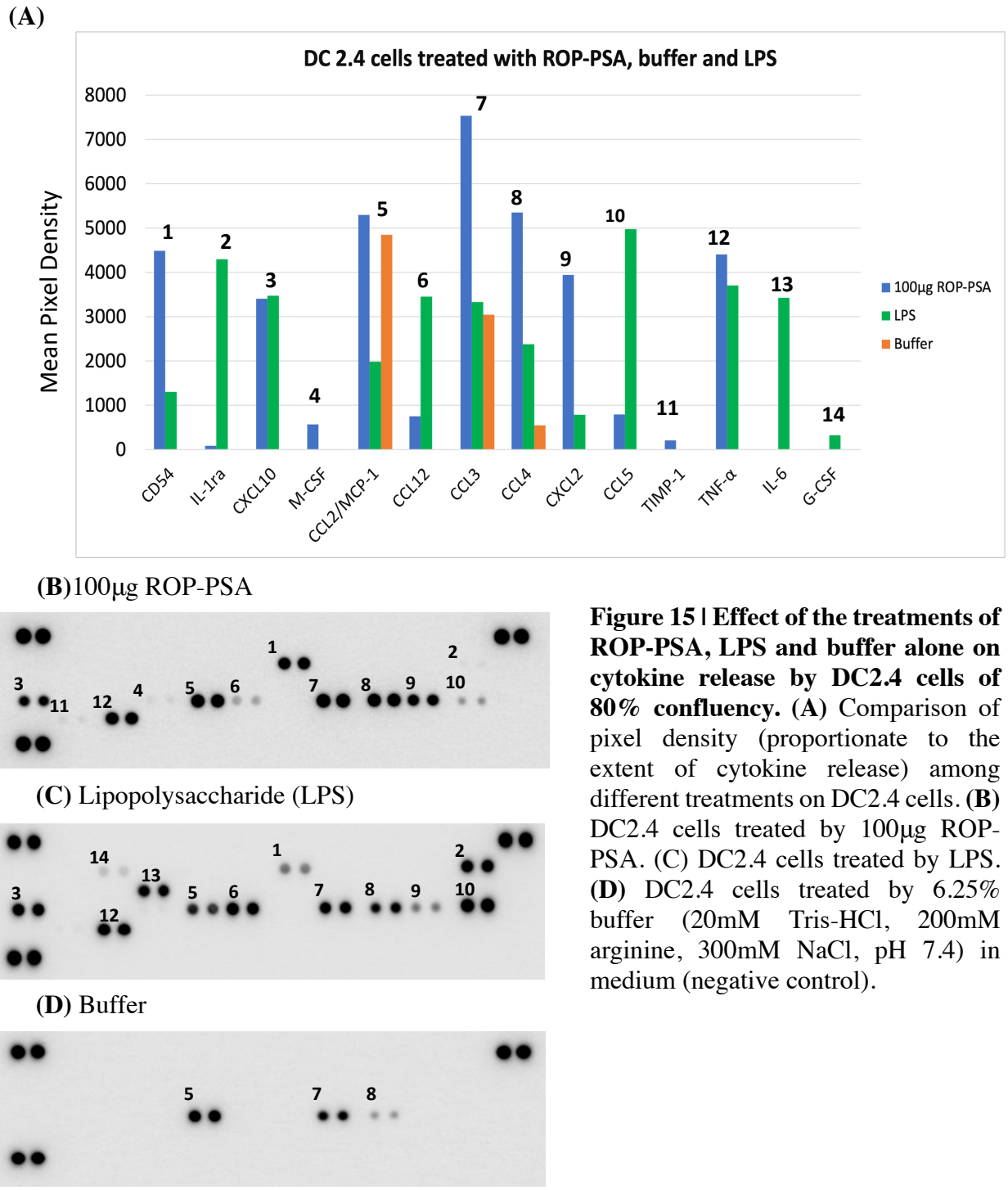

Figure 15 | Effect of the treatments of ROP-PSA, LPS and buffer alone on cytokine release by DC2.4 cells of 80% confluency. **(A)** Comparison of pixel density (proportionate to the extent of cytokine release) among different treatments on DC2.4 cells. **(B)** DC2.4 cells treated by 100µg ROP-PSA. (C) DC2.4 cells treated by LPS. **(D)** DC2.4 cells treated by 6.25% buffer (20mM Tris-HCl, 200mM arginine, 300mM NaCl, pH 7.4) in medium (negative control).

Figure 14 shows the coordinates on the cytokine array panel and their corresponding cytokine. The corner dots on the left side and upper right represent positive controls and the lower left represents a negative control. Each pair of duplicate spots represented each cytokine, whose average signal was determined for mean pixel density. Figure 15A shows the comparison of mean pixel density (proportionate to the extent of cytokine release) among different treatments (100 µg ROP-PSA, LPS and buffer) on DC2.4 cells. As

confirmed from the comparison between the cytokine profile of ROP-PSA (Figure 15B) and buffer (Figure 15D – negative control), ROP-PSA uptake triggered multiple cytokine and chemokine release by DC2.4 cells. The cytokine profile of ROP-PSA resembled that of LPS (Figure 15C). The level of CD54, CCL2, CCL3, CCL4, CXCL2, TNF-α release triggered by ROP was higher than that by LPS while it was the opposite for IL-1ra, CCL12 and CCL5. For CXCL10, it was approximately the same for both treatments. M-CSF and TIMP-1 release was triggered by ROP but not LPS, and LPS triggered IL-6 and G-CSF release while ROP did not.

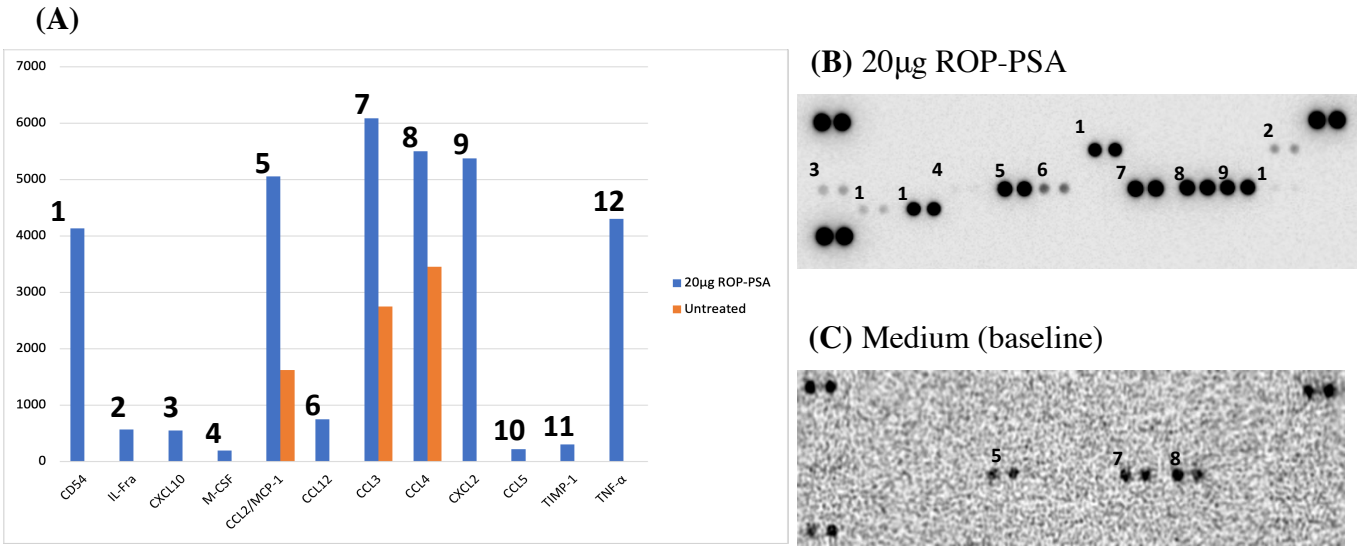

Figure 16 | Effect of the treatments of ROP-PSA compared with baseline on cytokine release by DC2.4 cells of 80% confluency. **(A)** Comparison of pixel density (proportionate to the extent of cytokine release) between ROP-PSA and medium on DC2.4 cells. **(B)** DC2.4 cells treated by 20µg ROP-PSA. **(C)** DC2.4 cells in cell culture medium.

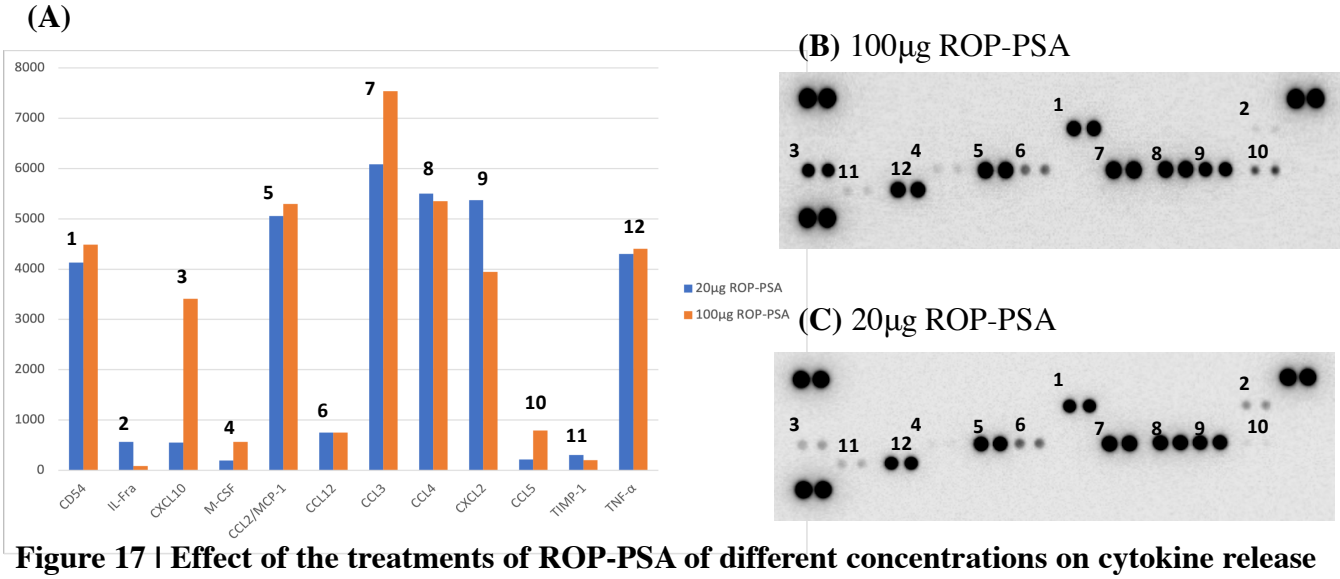

Figure 17 | Effect of the treatments of ROP-PSA of different concentrations on cytokine release by DC2.4 cells of 80% confluency. **(A)** Comparison of pixel density (proportionate to the extent of cytokine release) between 100µg (50ug/mL) ROP-PSA and 20µg (10µg/mL) ROP-PSA on DC2.4 cells. **(B)** DC2.4 cells treated by 100µg ROP-PSA. **(C)** DC2.4 cells treated by 20µg ROP-PSA.

The level of cytokine release represented by pixel density was compared between treatment with low concentration of ROP (20 µg) and baseline (Figure 17). Compared with baseline (buffer alone). 9 more cytokines were released following treatment with the lower concentration (10 µg/mL) of OVM300. In contrast, the pixel (level of cytokine secretion) was generally higher in higher dose (50 µg/mL) which concluded that cytokine release was proportionate to treatment dosage.

Endotoxin (LPS) level of 800µg/mL ROP-PSA sample was estimated to be 5.19 E.U. according to LPS quantification assay conducted by Yuqian Ou, a laboratory colleague, which was brought down to 0.65 E.U. in 100µg (Figure 15.B), whose concentration was at least $3.8x10^5$ times smaller in comparison with LPS sample used in the assays (5 µg/mL or $2.5x10^5$ – $5x10^5$ E.U. /mL) and thus indicated minimal effect on results.

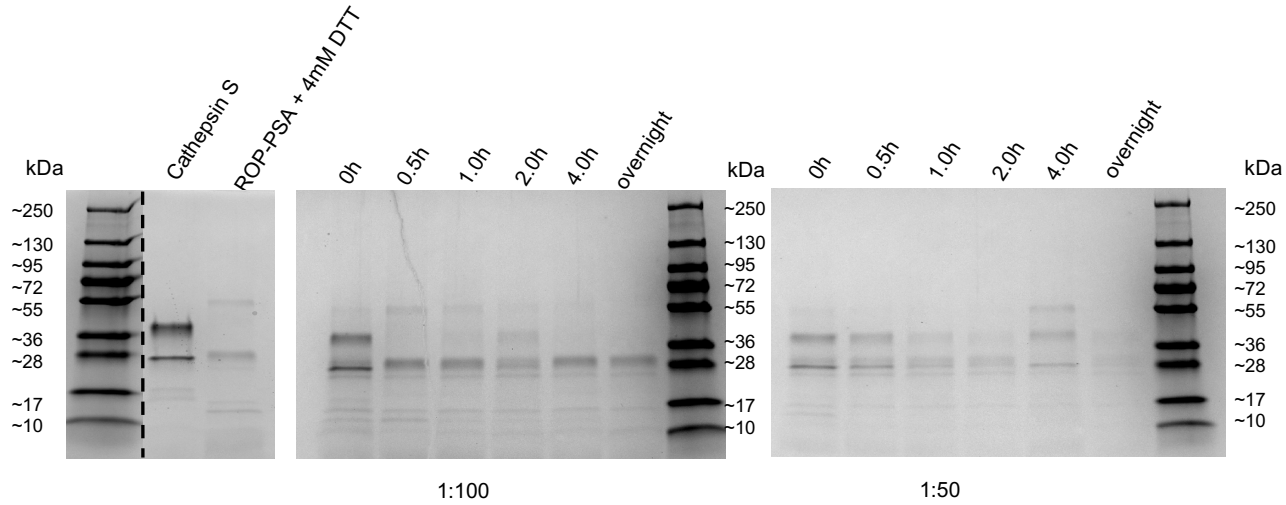

Figure 18 | ROP-PSA digestion by cathepsin S. Illustration of SDS-PAGE analysis as a result of overnight cathepsin S digestion using different cathepsin S to ROP-PSA ratio, 1:100 w/w and 1:50 w/w. Dotted line was applied to represent the digital removal of a part of a gel. SDS-PAGE gels were adjusted for parallel comparison.

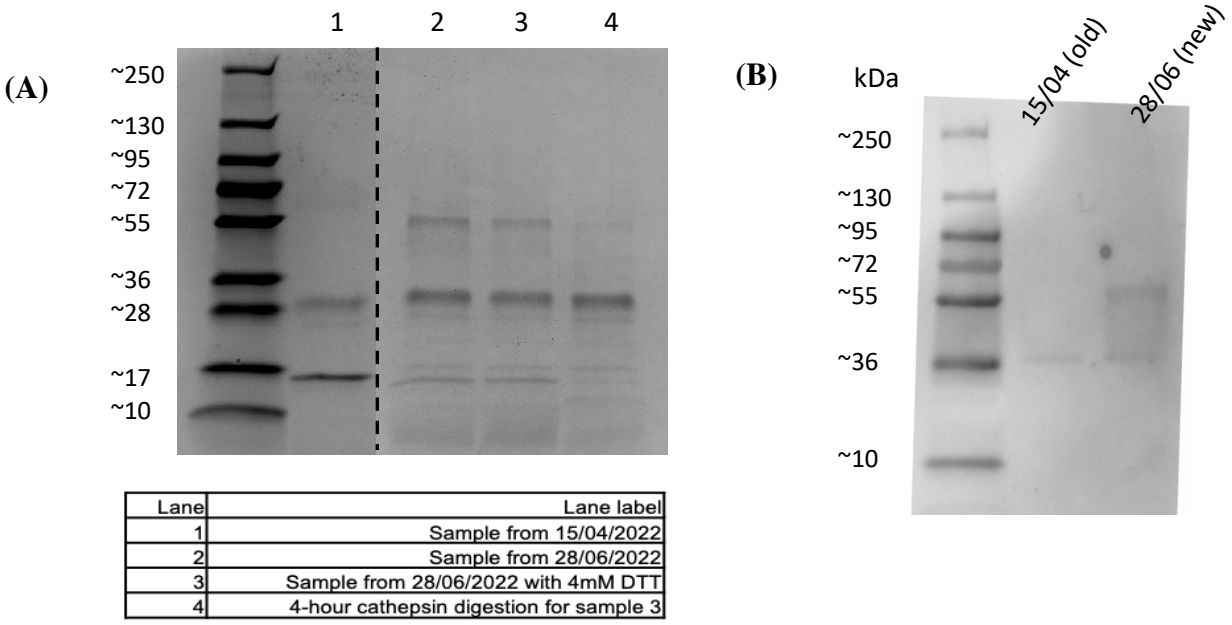

Lane	Lane label
1	Sample from 15/04/2022
2	Sample from 28/06/2022
3	Sample from 28/06/2022 with 4mM DTT
4	4-hour cathepsin digestion for sample 3

Figure 19 | ROP-PSA digestion by cathepsin S. (A) Illustration of SDS-PAGE analysis on two batches of OVM300 (a ROP-PSA product) at different time points and cathepsin S digestion on for the later batch. Dotted line was applied to represent the digital removal of a part of a gel. **(B)** Illustration of Western blot analysis on two batches of ROP-PSA at different time points.

Human cathepsin S was used in this protocol with 37 kDa of molecular weight (Figure 18), which should be the top band demonstrated on Figure 18-cathespsin S (91). The sample has shown signs of degradation due to storage. OVM300 with approximate 58 kDa was degraded during storage to a significant band at 28 kDa and down to 10 kDa. However for both 1:100 and 1:50, the top band disappeared gradually over time to bands of lower

molecular weights, especially in 1:100 where bands were more prominent due to higher concentration of OVM300. 100:1 w/w OVM300 at 4 hours was sampled for mass spectrometry analysis for optimal digestion at shortest time.

Figure 19 aimed to demonstrate the effect of storage on OVM300. As seen from SDS-PAGE (Figure 17.A), the band which represents the original sequence was barely present, remaining bands at 28-36 kDa and 10-17 kDa for the old batch, while full length was still present for the new batch with about two months apart. However his-tag was still intact with the band between 28 kDa and 36 kDa as shown on the western blot, while it has been proved cytokine release was successfully triggered with sample used from the new batch.

Investigating cathepsin S cleavage with mass spectrometry analysis

Band	Corresponding peptides from MASCOT protein library
A	ERPA_ECOBW K1C9_HUMAN
B	K1C9_HUMAN K22E_HUMAN FER_ECOLI ERPA_ECOBW
C	PTMA_BOVIN K1C9_HUMAN FER_ECOLI
D	SLYD_ECOLI K1C9_HUMAN
E	SLYD_ECOLI

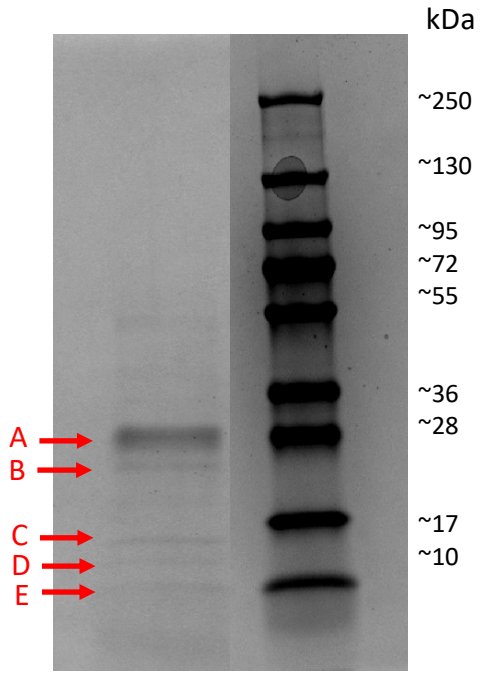

Same hits for A, B, D, E but no hits for C using OVM300 sequence analysis

```
  1 MHHHHHHENL YFQGMAPLIL SRIVGGWECE KHSQPWQVLV ASRGLRMKHS
 51 QPWQVLVASR GRAVCGGVLV HPQWVLLRMK RAVCGGVLVH PQWVLTAAHC
101 IRNKSVILLG LRMKTAAHCI RNKSVILLGR HSLFHPEDTG QVFQLRMKRH
151 SLFHPEDTGQ VFQVSHSFPH PLYDMSLLLR MKVSHSFPHP LYDMSLLKNR
201 FLRPGDDSSH DLLRMKKNRF LRPGDDSSHD LMLLRLSEPA ELTDAVLRMK
251 MLLRLSEPAE LTDAVKVMDL PTQEPALGTT LRMKKVMDLP TQEPALGTTC
301 YASGWGSIEP EEFLLRMKCY ASGWGSIEPE EFLTPKKLQC VDLHVISNLR
351 MKTPKKLQCV DLHVISNDVC AQVHPQKVTK FMLRMKDVCA QVHPQKVTKF
401 MLCAGRWTGG KSTCSGLRMK LCAGRWTGGK STCSGDSGGP LVCNGVLQGI
451 LRMKDSGGPL VCNGVLQGIT SWGSEPCALP ERPSLRMKTS WGSEPCALPE
501 RPSLYTKVVH YRKWIKDTIV ANP
```

Figure 20 | Tandem mass spectrometry analysis of 1:100 cathepsin S digestion at 4 hours under 37°C. Samples A-E were sent for MSMS analysis. The table shows the hits for all samples from MASCOT protein library, while A, B, D, E has the same sequence hit in OVM300 shown in red. No hits are present for sample C for OVM300. Cathepsin cleavage site – LRMK is bracketed in orange on the sequence.

Five band samples were sent for tandem MS analysis to investigate cathepsin S cleavage for OVM300 (Figure 20). The table shows peptides found in sample A to E from MASCOT protein library. Both K1C9_HUMAN and K22E_HUMAN are keratin proteins present in human skin tissue with a molecular weight of 64-65 kDa (92). ERPA_ECOBW and FER_ECOLI are both iron-sulphur protein found in *E. coli* and have a similar molecular weight of about 10 kDa, which are involved in a wide variety of metabolic reactions (93). SLYD_ECOLI of 21 kDa derived from *E. coli* is associated with preventing aggregation and promoting the correct folding of other proteins (94). PTMA_BOVIN stands for prothymosin

alpha of 12 kDa which can mediate immune function by conferring resistance to certain opportunistic infections. For lane A, B, D, E, same amino acid sequence hit LSEPAELTDAVLR (highlighted in red in Figure 20) was found in MSMS from OVM300 sequence while there was none for C. Results will be further commented on the discussion section.

Discussion

ROP-PSA expression and purification from *E. coli* expression system

Protocol optimisation for the purification of ROP-CTL-PSA

Given the formation of inclusion bodies, both products require strong denaturant to facilitate solubilisation of the inclusion bodies for purification. 8 M urea was initially used for this purpose in which a large proportion of target protein was solubilised. Denaturation was then conducted by the application of 6 M guanidine and both purity and concentration of the target protein was lower compared to urea (Figure 5). In summary 8 M urea is stronger in denaturing this ROP in this case.

Urea denatures protein by introducing a loss of water from the first solvation shell of protein due to electrostatic interaction and then an in-flow of itself toward the protein (95). Guanidine hydrochloride is an ionic denaturant and at high concentration (6 M) it acts as chaotropic agent to break down the structure of proteins (96). The ability in denaturation is dependent on electrostatic interactions with the individual protein. However, SDS-PAGE cannot be used for the analysis of guanidine-processed protein without ethanol precipitation.

Looking into the composition of ROP-CTL-PSA, above one fifth of amino acids is made up of cysteines which form inter- and intra-molecular disulphide bonds during oxidative folding between the thiol groups of residues. Although it is unlikely to calculate the number of disulphide bonds from the amino acid sequence of an artificial protein, the number of cysteine residues is proportionate to the number of unpaired free thiols which increase possibility of forming random disulphide bonds during refolding and producing covalent aggregates (97). In this case, a reducing agent, dithiothreitol (DTT) at 1 mM was used to break disulphide bonds and reduce insoluble aggregates during denaturation.

Ni-NTA Agarose was used for nickel affinity chromatography across two proteins. It is used to bind histidine residues in the 6xHis tag to the vacant positions in the coordination sphere of the immobilized nickel ions (98). Since a His-tag was not present in the sequence of ROP-CTL-PSA, nickel affinity chromatography was not able to capture target protein and vast majority of solubilised protein flew through the nickel column. Another purification method may need to be sourced e.g. ion exchange chromatography and size exclusion chromatography.

Protocol optimisation for the purification of OVM300

Comparison between E. coli, yeast, insect and mammalian cell expression systems

Both OVM300 and ROP-CTL-PSA were expressed in *E. coli* which are fast-grown at high cell density from readily available and affordable media. It is also efficient and straightforward to conduct transformation with exogenous DNA plasmids from as little as 5 minutes (99). BL21 cells as an *E. coli* strain are chosen as a host whose *hsd*SB mutation prevents plasmid loss and thus disrupts DNA methylation and degradation. However, the presence of outer membrane protease OmpT can induce digestion of extracellular proteins, especially during cell lysis (100). Also, the introduction of a foreign plasmid in *E. coli* results in the loss of the spatio-temporal control of its expression. Therefore the recombinant protein is expressed in the cytosol of *E. coli* whose pH, osmolarity, redox potential, cofactors and folding mechanisms are not controlled. Also, more hydrophobic groups are available for interactions in high concentration. These factors are contributory to the formation of insoluble inclusion bodies (101). There is also a risk of toxicity using bacteria to express proteins. To troubleshoot, protease inhibitor was added during sonication to hamper OmpT action on target protein. Denaturation with high concentration detergent was implemented to solubilise target protein out of inclusion bodies. Finally, endotoxin was removed to avoid toxicity in cell-based assays.

E. coli is usually the first host cell to be considered for recombinant protein development, accounting for 60% among all expression systems from 1995 to 2009 (102). Apart from bacteria, using yeast, insect, mammalian cells to express complex recombinant proteins is common too. Yeast as a eukaryotic cell, makes a remarkable system for the expression of recombinant eukaryotic proteins. It is also easy and fast to grow using fermentation (103). It was suggested by Bill, 2014 (104) to consider it as first choice host given the ability to screen for the expression of recombinant genes in both *E. coli* and yeasts. Mammalian systems seem to be the most straightforward answer for expressing mammalian proteins at its native state with complete biological activity. However, this application is expensive and requires complex technology and materials such as suitable cell lines and vectors (105), which may not be suitable in a simple laboratory setting. Last but not least, insect cells are suitable for high-yield expression similar to mammalian systems (106). Likewise, it requires a vector i.e. baculovirus and similar expertise; moreover, the expression levels vary between different proteins. For example, secreted glycoproteins i.e. PSA are usually expressed at a lower level (107).

Studies have shown that antigen glycosylation is important to facilitate antigen presentation by MHC I and II complexes (108). It can encourage antigen uptake by DC receptors which contain glycan-binding sites (109), influence proteolytic processing of protein antigens by blocking the action of proteases (110), and survive unintended lysosomal degradation (108). Therefore, it is important to maintain a certain level of wild-type glycosylation in ROP-PSA from the expression stage.

Glycosylation was generally considered to happen in eukaryotes. Mammalian systems especially are advantageous for the production of human type glycans for functional interaction with human cells but are seldomly used in laboratory settings due to cost and

susceptibility to viral and bacterial infections (111). However, there are however a few strategies to engineer *E. coli* to increase the efficiency of glycoprotein production in *E. coli*. The codon optimisation of *PglB* from *C. jejuni* has been shown to increase glycosylation significantly by accepting and transferring the eukaryotic core glycan to target proteins (112). Other than that, inverse metabolic engineering through high throughput screening using soybean agglutinin peroxidase reactions is also helpful by reducing the metabolic burden to the host (113). With these recent advances, the future of industrial glycoprotein production from E. coli seems very bright.

Increasing protein solubility

While it is mostly inevitable for recombinant proteins to become insoluble because of misfolding when overexpressed in a heterologous host e.g. *E. coli* (114) related to hydrophobic residues on the surface of the protein, there are strategies to increase soluble expression of recombinant proteins. Apart from altering expression conditions, solubility-enhancing fusion tags e.g. *E. coli* thioredoxin, *E. coli* nusA, and maltose binding protein (114), are widely used at the plasmid design stage to increase the pure yield of soluble protein and peptide's immunogenicity (115). Another strategy to prevent the formation of inclusion bodies is the co-expression of molecular chaperones. Exposed hydrophobic residues on the surface of the protein can be protected by unintended inter- or intramolecular interactions with these chaperones (116).

Here a strong detergent (urea) was used to denature the protein at high concentration and therefore solubilise the inclusion bodies. The solubilising buffer contained 8M urea, 1mM DTT, 300mM NaCl and 20mM Tris-HCl at pH 8.0. Sodium chloride was used in low concentration (1.755%) to increase the solubility of the protein by increasing the ionic strength of the solution and decreasing the electrostatic energy between the protein

molecules. This is called the salting in effect. DTT is a reducing agent used in protein purification to reduce the disulphide bonds in the protein structure. 1mM DTT was used first but the yield and purity were unsatisfactory given the significant amount of cysteine residues in OVM300. 2mM DTT was used afterwards to increase the efficiency of breaking disulphide bonds. According to the SDS-PAGE gel, the purity and concentration of OVM300 under 2mM DTT treatment were visibly higher than that under 1mM DTT. However, the tolerability for nickel resins was not more than 5mM. Experience informed 2mM DTT could already aggressively reduce nickel ions and undermine the binding capacity of the column. Balancing benefits and risks, no higher concentration of DTT was used. It was also interesting to notice a remarkable band at ~36 kDa on lane 4 (Figure 7). A western blot was conducted later (Figure 9 lane 2) to confirm the expression of a truncated version of OVM300 by using anti-polyHistidine as antibody. Nevertheless, it was also possible to be the case of non-specific binding to the antibody due to the excessive amount of protein (impurities).

Optimising nickel affinity chromatography – increasing protein yield and purity

Recombinant protein can be eluted from a nickel column by imidazole, lowering pH, or using strong chelating agents such as EDTA and EGTA. Here a high concentration of imidazole was used, which is usually the most common method. Imidazole acts as a competitive agent with protein binding to nickel resins. It is used as a wash buffer with a low concentration to wash out weakly-bounded protein (117) and thus increase the final purity. Target protein is usually eluted out at a concentration gradient. This however is a trial and error process to find out the optimal imidazole concentration for to achieve highest yield as it is protein dependent and must be established on each case (118).

Figure 8 outlined the difference in yield and purity between batch spin method and gravity flow method. Gravity flow was superior in both parameters and thus was used subsequently.

However, experience showed it was more time-consuming with OVM300 given the high concentration and high impurity level of the denaturation supernatant. This is a common limitation in manual column loading and can be improved by passing through a 0.22μM filter and increasing sonication speed or time (119). Both methods have been tried: protein yield significantly decreased with filtration but the solution became visibly less viscous with increasing sonication time from 5 seconds to 10 seconds each cycle for 60 cycles. Going forward with increased sonication time, centrifugation time was also increased from 20 minutes to 30 minutes to enhance precipitation of insoluble protein, which in turn reduced the viscosity of the loading solution. According to results from Figure 8, 10% solution B (48mM imidazole) was used as washing buffer to remove weakly-bounded protein impurities; 60% solution B (188mM imidazole) was used as elution buffer to collect OVM300; 100% solution B (300mM imidazole) was used to wash out all remaining bound protein from the column. Nickel resins can be reduced and deactivated by DTT so it is suggested to reduce repetitive use of nickel resins and recharge them regularly. There are also alternatives for DTT such as β-mercaptoethanol (BME) and tris(2-carboxyethyl) phosphine (TCEP) to maintain disulphide bond breakage. BME and TCEP are both reducing agents and not as aggressive as DTT. However TCEP is expensive and may not be suitable for protocol optimisation. BME is worth trying as it is more stable than DTT but it is less reducing (redox potential -0.26V vs. -0.33V) so higher concentration needs to be used (98,120).

Optimising refolding – reactivating protein

During denaturation, aggregated forms of protein present in inclusion bodies is dissolved in high concentration denaturant i.e. 8M urea which is used to reduce the non-covalent interactions between protein molecules (e.g. hydrogen bonds) so that the protein becomes unfolded. Therefore, the removal of denaturant theoretically refolds the protein to its biologically active forms (121). However the possibility of off-pathway reactions may lead to

the formation of aggregates (122). The refolding method used in this project was step-wise dialysis where a gradual removal of denaturant was performed as opposed to sudden drop of denaturant concentration in one-step dialysis, preventing significant misfolding and protein aggregation (121). Stepwise analysis, however, is a time-consuming process as well as a trial-and-error procedure in protocol optimisation.

Table 2 outlined the refolding recipes used for optimisation. Generally, apart from urea and DTT whose uses have been covered above, other chemical additives were used to assist solubilisation and refolding. Tween-80, a non-ionic surfactant, was added (Table 2C) as it is thought to reduce protein adsorption and stabilize the protein (123) while removed afterwards due to significant cytotoxicity at such high concentration (124). Sarkosyl is a mild detergent that serves the same purpose as urea and was added at initial stage of refolding to replace the stronger detergent to avoid misfolding. Its concentration was reduced gradually to zero at end stage (125) due to cytotoxicity (Figure 10A). Arginine or L-arginine which is a natural occurring amino acid, is classified as a protein aggregation inhibitor. This was added to the second step of the refolding process to prevent aggregation of partially folded intermediates by its possible interaction with water molecules and protein (126,127). Reduced and oxidized form of glutathione i.e. GSG/GSSG was used instead of DTT during optimisation because it promotes disulphide exchange instead of only breaking disulphide bonds, which is effective in the formation of secondary and tertiary structure (128). Apart from additives, it is worth noting that maintaining stirring and its speed is important during refolding process to ensure efficient dialysis. Stirring was stopped on some occasions due to mislocation of the dialysis bag and technical errors. The environmental-based disturbance led to structural perturbation and thus formation of aggregated species (122). At the end of the optimisation, the recovery level reached 100% (clear protein solution) before pH adjustment. pH was adjusted to 7.4 (Table 2I), where the resultant recovery dropped to 30%.

This indicates pH is a crucial factor for protein solubility; however, the adjustment was also essential for biocompatibility.

Results (Figure 10) were taken into consideration what to add to the refolding buffer while the experiment for Figure 12 was the investigation for the general cytotoxicity the refolding buffer has on DC2.4 cells. Figure 12B showed that the refolding buffer was biocompatible at lower concentration from 12.5% and suggested its suitability in subsequent cell-based cytokine array assays.

Effects of storage and freeze-thawing process on ROP-PSA

Figure 19B showed the degradation of the band at ~55 kDa after storage and repeated freeze-thawing process. This can potentially affect protein stability. To optimise the freezing-thawing protocol, Cao E, et al. (45) advised that it was preferable for protein to undergo slow freezing (about 1^{o}C/min) and fast thawing (>10 ^{o}C/min) process in order to avoid exposure to ice-liquid interface and additional interfacial tension during recrystallization (129). Also, lowering the salt concentration of the buffer decreases precipitation and helps improve the activity recovery of proteins (130). The western blot however, confirmed the main truncated protein band at ~36 kDa was part of the original sequence. Further investigation is required by mass spectrometry to investigate the cleavage. Immunogenicity of the vaccine should not be affected if the cleavage site is cathepsin S protease specific instead of between one of the T cell-specific epitopes.

Cytokine and chemokine release upon ROP-PSA uptake

Comments on aim and hypothesis

Cytokines and chemokines are small soluble proteins that orchestrate intercellular communications within the immune system to regulate inflammation, proliferation,

differentiation, metabolism, chemotaxis and tissue repair (131). They can serve as products and/or inducers of differentiation of DCs (132). DCs can be activated by a variety of antigens such as microorganisms and dead lysate through interaction between pathogen-associated molecular patterns (PAMPs) and pattern-recognition receptors (PRRs) as well as through phagocytosis. This research project mainly investigates the cytokines and chemokines produced by DC2.4 cells upon ROP-PSA uptake. We hypothesized that exposure to ROP-PSA, secretion of pro-inflammatory cytokines was triggered upon antigen uptake. Mouse Cytokine Array Kit used in this project is a membrane-based antibody array, where each membrane is spotted in duplicate with 40 different cytokine antibodies, for the determination of the relative levels of such cytokines and chemokines in cell culture supernatants, while it is also applicable to cell lysates, tissue lysates, serum, and plasma (88). Murine bone marrow-derived DC2.4 cells are an immortal cell line used in this experiment. It represents critical features of DCs including the expression of DC-specific markers, and the ability to phagocytose (133).

Comments on experiment design and limitations

Five samples were used in this experiment including: a higher (100μg/mL) and lower (20μg/mL) concentration of OVM300, the solubilising buffer of the same volume of the higher concentration of OVM300 as negative control, cell culture medium alone (baseline), and liposaccharide (LPS). LPS is commonly derived from bacteria in this case and remain in *E. coli* derived protein after purification if not properly removed. According to LPS quantification assay, its level is minimal in purified sample compared with LPS used in this assay. Moreover, by comparing the differences between their cytokine profiles, it is safe to suggest the results are reliable.

It was however not a time-course experiment where only a snapshot of cytokine expression was captured i.e. after overnight incubation. The experiment mainly investigates upstream immune responses e.g. DC maturation and activation and the potential of antigen-induced cytokine/chemokine release for T cell activation and downstream immune response as no other cells apart from DC2.4 were used for interactions. One of potential limitations of this study is that the peptide is of human origin but the cell line is murine. Despite considerable similarities between human and murine DCs in terms of development and functions, cautious measures should be taken in interpreting results as physiological mechanisms might not be conserved (134,135). However, the cytokine release profile generated from this study is still significantly useful for pre-clinical murine studies.

Analysis for cytokine release profile

Figure 15 shows OVM300 (ROP-PSA) incubation with DC2.4 cells overnight was able to trigger release of 12 different cytokines and chemokines on the array. LPS was used as positive control. Table 4 outlined the cytokine profile for ROP-PSA, LPS and buffer and their general functions in the immune system. G-CSF, M-CSF and tumour necrosis factor-α (TNF-α) are crucial in the stimulate on of DC maturation (136). TNF-α is a cytokine which is both pro- and anti-inflammatory, mediating both cell death and cell survival dependent on its time and place in the immune response. However, TNF-α release by DC coordinates the activation of both CD4+ and CD8+ T cells, including upregulating IL-2R and other cytokines and facilitating proliferation (137). CD54 overexpression is a sign of DC activation and is one of the co-stimulatory molecules that interact T cells to enhance adhesion and signalling (136). It was used as a potency measure of sipuleucel-T for assessing human APC activation (138). A variety of chemokines is produced by DC2.4 upon ROP-PSA uptake including: CXCL2, CXCL10, CCL2, CCL3, CCL4, CCL5 and CCL12. They function mainly as chemoattractant for leukocytes, recruiting and directing monocytes, neutrophiles and

other effector cells to sites of inflammation. CCR5 ligands CCL3 and CCL4 produced by DCs recruits naïve CCR5-expressing CTLs for cross priming, which is sustained throughout antigen-specific interaction between DCs and T-helper cells (139,140). IL-1ra is a secreted anti-inflammatory cytokine and inhibits the pro-inflammatory effect of IL-1 by binding to their common activating receptor IL-1ra. Murine studies concluded that the upregulation of such cytokine was favoured in mice in relation to IL-1, its pro-inflammatory form (141). DC2.4 cells used in this study are derived from C57BL/6 mice which are considerably more tolerable of IV-administered RNA vaccine than humans (142). Further investigation is needed to address whether the same situation applies to peptide vaccines and if they produce different cytokine profiles.

Cytokine	Induced by	Function
CD54/ ICAM-1	• ROP-PSA • LPS	○ Glycoprotein - upregulated in case of DC activation. ○ Stabilize cell-cell interactions and facilitate leukocyte endothelial transmigration
IL-1ra	• ROP-PSA • LPS	○ Natural inhibitor of the pro-inflammatory effect of IL1
CXCL10	• ROP-PSA • LPS	○ Chemoattraction for monocytes/macrophages, T cells, NK cells, and dendritic cells ○ Promotion of T cell adhesion to endothelial cells ○ Antitumor activity ○ Inhibition of bone marrow colony formation ○ Angiogenesis
M-CSF	ROP-PSA	Proliferation, differentiation, and survival of monocytes, macrophages, and bone marrow progenitor cells
CCL2	• ROP-PSA • LPS • Buffer	Recruit monocytes, memory T cells, and dendritic cells to the sites of inflammation produced by either tissue injury or infection.
CCL12	• ROP-PSA • LPS	Attract eosinophils, monocytes and lymphocytes.
CCL3	• ROP-PSA • LPS • Buffer	Recruit and activate of polymorphonuclear leukocytes through binding to the receptors CCR1, CCR4 and CCR5
CCL4	• ROP-PSA • LPS • Buffer	○ Macrophage inflammatory protein-1β (MIP-1β) ○ Specific for CCR5 receptors ○ Chemoattractant for natural killer cells, monocytes and other immune cells
CXCL2	• ROP-PSA • LPS	○ Powerful neutrophil chemoattractant ○ Involved in many immune responses including wound healing, cancer metastasis, and angiogenesis.
CCL5	• ROP-PSA • LPS	○ Proinflammatory chemokine, recruiting leukocytes to the site of inflammation ○ Chemotactic for leukocytes ○ Induce the proliferation and activation of certain NK cells to form CC-Chemokine-activated killer cells
TIMP-1	ROP-PSA	The glycoprotein is a natural inhibitor of the matrix metalloproteinases (MMPs), a group of peptidases involved in degradation of the extracellular matrix.

TNF-α	• ROP-PSA • LPS	Inflammatory cytokine produced by macrophages/monocytes during acute inflammation and is responsible for a diverse range of signaling events within cells, leading to necrosis or apoptosis.
IL-6	LPS	○ IL-6 is secreted by macrophages in response to PAMPs ○ Stimulate acute phase protein synthesis, as well as the production of neutrophils in the bone marrow. ○ Support the growth of B cells and is antagonistic to regulatory T cells.
G-CSF	LPS	Stimulates the survival, proliferation, differentiation, and function of neutrophil precursors and mature neutrophils.

Table 3 | Cytokine and chemokine release profile induced by different antigens i.e. ROP-PSA, LPS and refolding buffer alone (20mM Tris-HCl pH 7.4, 300mM NaCl, 200mM arginine), and their functions, adapted from Janeway's Immunology (73)**.**

How ROP-PSA overcomes challenges in peptide vaccines

The main challenges in peptide-based vaccines include low immunogenicity, immune evasion and HLA allotype restriction (44). To ensure clinical efficacy in peptide vaccines, it must be able to be expressed by dendritic cells (or antigen-presenting cells), trigger CD4+ helper T cell and CD8+ cytotoxic T cell responses. CD4+ T cells are critical to activate and sustain effector CTL activity, as well as intensify long-term antitumour activity, epitope spreading and tumour infiltration (44). Available data suggested that almost all human DC subsets have some ability to cross present soluble proteins on MHC I molecules taken into account of the type of antigen, stimulatory factors, timing of antigen entry and stage of immune response. CD8+ T cells are crucial for targeting cancer. After being primed by DCs, they are differentiated to form effector CTLs to kill cancer cells presenting MHC I molecules through release of granules or induction of apoptosis (143). CD4+ T cells have an intertwined relationship with CD8+ T cells in anti-tumour immunity. The secretion of interleukin (IL)-2 by activated CD4+ T cells directly facilitates the effector function, differentiation, and proliferation of CD25+ CD8+ T cells (144,145). By sustaining pro-inflammatory cross-presenting DCs, CD4+ T cells indirectly provide the three activating signals (MHC I/peptide/TCR, CD28/B7 costimulatory signals, IL12 release) for CTLs by upregulation of CD40 ligand (146,147). Apart from that, the production of effector cytokines such as IFNγ and TNFα by polarised CD4+ T_H1 cells provides direct anti-tumour activity

(148). ROPs harnesses the ability of DC cells to present MHC II and cross-present MHC I to prime/activate naïve CD4+ and CD8+ T cells respectively.

Peptide based vaccines are usually delivered as a pool of shorter peptides or synthetic long peptide. Both correlate with HLA-subtype restriction due to lack of diversity required for high polymorphism of HLA (149) while shorter peptides are rapidly cleared from the body for the tendency of enzymatic digestion (150). The delivery of a whole protein allows DC processing. Synthetic long peptides (SLPs) derived from 25-35 amino acid peptides of a tumour specific antigen however depend upon processing, which is limited to presentation by APCs (151). They demonstrated superior immunogenicity compared to whole wildtype antigen in terms of more efficient antigen presentation by DCs, increased CD4+ and CD8+ T cell activation (152). Murine studies using MELOE-1 as model antigen showed an improvement of epitope of processing and DC presentation due to an artificial separation of MHC I and MHC II epitopes with a cathepsin protease sensitive linker, resulting in a reduction in tumour growth in 4 out of 7 mouse tumour models (153). Both shorter peptides and SLPs are inferior in the activation of CD4+ response (34,153), hampering an all-round immunogenicity. Eventually, the design of ROP-PSA takes these into account and is adjusted for both proteasomal degradation and cathepsin S digestion (non-specific and specific digestion) by inserting LRMK linker (cathepsin S digestion site) between each 30-amino acid sequence (to be chopped by proteasome to peptides which are suitable for either MHC I or II loading).

Figure 18 showed gradual digestion of ROP-PSA with addition of cathepsin S incubated at 37°C overnight. SDS-PAGE gel was then sent to mass spectrometry analysis. Tandem MS (MSMS) showed peptide sequence hits from MASCOT protein library and OVM300. ERPA_ECOBW, FER_ECOLI, and SLYD_ECOLI are all proteins derived from *E. coli* which can be explained as evidence of the existence of the purified protein. However, the presence of human keratin protein showed the possibility of impurities from handling. It is notable that

sample C does not have any hits from OVM300 while has three hits from MASCOT library, with one of which bovine derived PTMA_BOVIN which is commonly used in tissue culture. This could suggest the existence of remaining cathepsin S protease. In general protein samples sent were in low concentration due to storage and freeze-thaw cycles. However, one hit on OVM300 sequence (LSEPAELTDAVLR) was found that is between two cathepsin cleavage sites which suggested *in vitro* that OVM300 can be digested by cathepsin S.

Potential of ROP-PSA for clinical use

Exploring potential as monotherapy

OVM200 which is an ROP-based vaccine targeting survivin over-expressed in most solid tumours including lung, breast, prostate and ovarian cancers, has been approved by MHRA to roll out first-in-men phase I clinical trials to investigate safety and efficacy in humans (154). This calls for the potential of OVM300 (ROP-PSA).

Optimal delivery and formulation

The assistance of adjuvants and ideal delivery vehicles in formulation is generally required for peptide-based therapies like ROP-PSA to induce cell-mediated immunity (44). To achieve cytotoxic T cell anti-tumour response, three kinds of signals are essential for the therapy to activate naïve T cells by antigen-presenting cells: binding of MHC:peptide to T cell receptor, co-stimulatory signal delivered by dendritic cells, cytokine release to direct T cell differentiation (73). Conjugates should be able to help with one or more of these mechanisms. Commonly used immune stimulation adjuvants include montanide ISA 51, GM-CSF and toll-like receptor (TLR) agonist. Subcutaneous injection with montanide ISA 51 augment uptake of antigen by local DCs due to its non-absorbable mineral composition and thus persist antigen presentation for T-cell priming (155). Granulocyte-macrophage colony stimulating factor (GM-CSF) has been commonly used in peptide-based cancer

vaccines in clinical trials (40,156) which is a growth factor for the recruitment, maturation and activation of dendritic cells (157). Preliminary results from this project also showed increased GM-CSF release by DCs upon ROP-PSA uptake, which is beneficial for maintaining lymphocyte activation. TLR agonist is useful for avoiding T-cell exhaustion and potentiate the efficacy of active ingredient (158). Optimising formulation is crucial for pharmacokinetics. Formulating with liposomal nanoparticles not only increases solubility and slows down elimination, but also was found to significantly enhance the epitope-specific anti-tumour immune response in *in situ* studies (159).

Exploring potential in combination therapy

The similarity of the cytokine release profile between ROP-PSA and LPS suggested a possibility of ROP-PSA to be a safer alternative to LPS in vaccine formulation. It can be used in combination with other tumour specific antigen e.g. PSMA and PAP. Lipopolysaccharide (LPS) is another example which signals through toll-like receptors (TLRs) to induce activation and maturation of dendritic cells despite holding remarkable toxicity (160) while its chemically detoxified form MPL is approved in human papillomavirus vaccines (161). TLR-4 activation by MPL results in mild inflammation which promote Th1 differentiation and its related humoral responses (162).

Apart from harnessing adjuvants to increase immunogenicity, ROP-PSA also holds potential for combination therapy with immune checkpoint inhibitors, conventional chemotherapies, and radiotherapy. In advanced prostate cancers, combinatorial aggressive treatments are usually the ideal methods for avoiding dose-dependent toxicities and encouraging efficacy as well as overcoming immunosuppressive tumour microenvironment (44,163). Immune checkpoint inhibitors (e.g. anti-PD1, anti-CTLA-1) work in the downstream of antitumour immune response by prolonging antigen-specific T cell action while peptide vaccines work

in upstream for immune-priming. On the other hand, pre-treatment of chemotherapy or radiotherapy induces apoptosis and release of tumour neo-antigen which thus help mature more DCs for CD8+ T cells cross presentation (164). Immunocompatible cytotoxic chemotherapy combined with immunotherapy has been a new approach in cancer therapy nowadays. The release of damage-associated molecular patterns (DAMPs) triggered by chemotherapy-induced cancer cell death potentiate the activation of APCs and especially NK-cell-lysis-induced DC maturation(165). Moreover, via the activation of different complementary pathways e.g. cGAS/STING pathway, chemotherapy can provide a synergistic effect with immunotherapy through activation of CTLs, depletion of Tregs and increased infiltration of CD4+ and CD8+ lymphocytes (165). For instance, docetaxel as a standard chemotherapy for mCRPC has been demonstrated to diminish immunosuppression by downregulating T reg cells (166) and proved superior in combination with a peptide-based vaccine and dexamethasone in a phase II clinical trial (167). *In vitro* studies also showed non-mutated neoantigens were generated by cisplatin-induced apoptotic tumour cells which elicited both CD4+ and CD8+ response by DC antigen presentation (164). Neoantigens are essentially tumour specific antigens which are only present in tumour cells (168). Therefore, by activating its release, chemotherapy can potentially reduce HLA-type restriction and then facilitate a well-rounded immune response. Combination with radiotherapy works by the same mechanism regarding releasing DAMP by cancer cell death.

Conclusion and future directions

This project has provided preliminary *in vitro* results for a recombinant peptide-based vaccine OVM300 (ROP-PSA) regarding its immunogenicity upon mouse-derived dendritic cells uptake based on its cytokine release profile. This represents a robust foundation for pre-clinical murine studies. Further attempts can be conducted to perfect protein purification via the use of fast protein liquid chromatography to increase yield and purity in terms of mass

production. With regards to preclinical studies, it is worth to compare the efficacy and safety in vivo between mRNA-based formulation and peptide-based formulation given the significant potential mRNA vaccines showed in recent years. For future directions, the design of the vaccine can be expanded to other different tumour specific antigens e.g. PAP and PSMA which are also overexpressed self-antigen in PCa cells. Overall recombinant overlapping peptides are attractive for PCa cancer vaccine design to induce T cell response in response to DC activation, which makes this technology a desirable candidate especially in combination therapy with chemotherapy and immune checkpoint inhibitors.

Acknowledgements

I would like to thank the following people, without whom I would not have been able to complete this research, and without whom I would not have made it through my masters degree!

My supervisors Professor Shisong Jiang and Dr Demin Li whose insight and knowledge into the project guided me through this research.

The Jiang's Lab at University of Oxford, Yuqian Ou, Alexander Stephens, Constantinos Demetriou and Sichen Liu, who have provided me practical help on experiments, insights and knowledge into the project and mental support in the laboratory.

My coursemates, aka the basement angels, Teofanija Trajanovska, Alexandra Loedin, Minn-E Ng, Aiyan Yau, and Kelly Lee, whose mental support helped me get through this stressful academic year.

And thanks to my friends Cheng I Chou, Maria Jeleń, Stella Elgood-Field and Hannah Grey, and my therapist Ruth Day for all the mental security you have given me throughout this year and keeping me sane.

Reference

1. Rawla P. Epidemiology of Prostate Cancer. World J Oncol. 2019 Apr;10(2):63–89.

2. Prostate cancer statistics [Internet]. Cancer Research UK. 2015 [cited 2022 Feb 17]. Available from: https://www.cancerresearchuk.org/health-professional/cancer-statistics/statistics-by-cancer-type/prostate-cancer

3. Cancer of the Prostate - Cancer Stat Facts [Internet]. SEER. [cited 2022 Aug 8]. Available from: https://seer.cancer.gov/statfacts/html/prost.html

4. PDQ Adult Treatment Editorial Board. Prostate Cancer Treatment (PDQ®): Health Professional Version. In: PDQ Cancer Information Summaries [Internet]. Bethesda (MD): National Cancer Institute (US); 2002 [cited 2022 Aug 9]. Available from: http://www.ncbi.nlm.nih.gov/books/NBK66036/

5. Merriel SWD, Pocock L, Gilbert E, Creavin S, Walter FM, Spencer A, et al. Systematic review and meta-analysis of the diagnostic accuracy of prostate-specific antigen (PSA) for the detection of prostate cancer in symptomatic patients. BMC Med. 2022 Feb 7;20(1):54.

6. Ilic D, Djulbegovic M, Jung JH, Hwang EC, Zhou Q, Cleves A, et al. Prostate cancer screening with prostate-specific antigen (PSA) test: a systematic review and meta-analysis. BMJ. 2018 Sep 5;362:k3519.

7. Fenton JJ, Weyrich MS, Durbin S, Liu Y, Bang H, Melnikow J. Prostate-Specific Antigen-Based Screening for Prostate Cancer: Evidence Report and Systematic Review for the US Preventive Services Task Force. JAMA. 2018 May 8;319(18):1914–31.

8. Naji L, Randhawa H, Sohani Z, Dennis B, Lautenbach D, Kavanagh O, et al. Digital Rectal Examination for Prostate Cancer Screening in Primary Care: A Systematic Review and Meta-Analysis. Ann Fam Med. 2018 Mar;16(2):149–54.

9. Systematic review of complications of prostate biopsy - PubMed [Internet]. [cited 2022 Aug 9]. Available from: https://pubmed.ncbi.nlm.nih.gov/23787356/

10. Resnick MJ, Koyama T, Fan KH, Albertsen PC, Goodman M, Hamilton AS, et al. Long-term functional outcomes after treatment for localized prostate cancer. N Engl J Med. 2013 Jan 31;368(5):436–45.

11. The Eighth Edition AJCC Cancer Staging Manual: Continuing to build a bridge from a population-based to a more ‘personalized’ approach to cancer staging - PubMed [Internet]. [cited 2022 Aug 9]. Available from: https://pubmed.ncbi.nlm.nih.gov/28094848/

12. Castration-resistant prostate cancer: Treatments targeting the androgen pathway - UpToDate [Internet]. [cited 2022 Aug 9]. Available from: https://www.uptodate.com/contents/castration-resistant-prostate-cancer-treatments-targeting-the-androgen-pathway?topicRef=6937&source=see_link#H1385299369

13. Fizazi K, Tran N, Fein L, Matsubara N, Rodriguez-Antolin A, Alekseev BY, et al. Abiraterone plus Prednisone in Metastatic, Castration-Sensitive Prostate Cancer. N Engl J Med. 2017 Jul 27;377(4):352–60.

14. Chi KN, Agarwal N, Bjartell A, Chung BH, Pereira de Santana Gomes AJ, Given R, et al. Apalutamide for Metastatic, Castration-Sensitive Prostate Cancer. N Engl J Med. 2019 Jul 4;381(1):13–24.

15. Davis ID, Martin AJ, Stockler MR, Begbie S, Chi KN, Chowdhury S, et al. Enzalutamide with Standard First-Line Therapy in Metastatic Prostate Cancer. N Engl J Med. 2019 Jul 11;381(2):121–31.

16. Kyriakopoulos CE, Chen YH, Carducci MA, Liu G, Jarrard DF, Hahn NM, et al. Chemohormonal Therapy in Metastatic Hormone-Sensitive Prostate Cancer: Long-Term Survival Analysis of the Randomized Phase III E3805 CHAARTED Trial. J Clin Oncol Off J Am Soc Clin Oncol. 2018 Apr 10;36(11):1080–7.

17. Fizazi K, Maldonado X, Foulon S, Roubaud G, McDermott RS, Flechon A, et al. A phase 3 trial with a 2x2 factorial design of abiraterone acetate plus prednisone and/or local radiotherapy in men with de novo metastatic castration-sensitive prostate cancer (mCSPC): First results of PEACE-1. J Clin Oncol. 2021 May 20;39(15_suppl):5000–5000.

18. Thomas C, Baunacke M, Erb HHH, Füssel S, Erdmann K, Putz J, et al. Systemic Triple Therapy in Metastatic Hormone-Sensitive Prostate Cancer (mHSPC): Ready for Prime Time or Still to Be Explored? Cancers. 2021 Dec 21;14(1):8.

19. Patient education: Treatment for advanced prostate cancer (Beyond the Basics) - UpToDate [Internet]. [cited 2022 Aug 9]. Available from: https://www.uptodate.com/contents/treatment-for-advanced-prostate-cancer-beyond-the-basics#H18328116

20. Madan RA, Arlen PM, Mohebtash M, Hodge JW, Gulley JL. Prostvac-VF: a vector-based vaccine targeting PSA in prostate cancer. Expert Opin Investig Drugs. 2009 Jul;18(7):1001–11.

21. Cunha AC, Weigle B, Kiessling A, Bachmann M, Rieber EP. Tissue-specificity of prostate specific antigens: Comparative analysis of transcript levels in prostate and non-prostatic tissues. Cancer Lett. 2006 May 18;236(2):229–38.

22. Balk SP, Ko YJ, Bubley GJ. Biology of Prostate-Specific Antigen. J Clin Oncol. 2003 Jan 15;21(2):383–91.

23. Graddis TJ, McMahan CJ, Tamman J, Page KJ, Trager JB. Prostatic acid phosphatase expression in human tissues. Int J Clin Exp Pathol. 2011 Mar;4(3):295–306.

24. Ghosh A, Heston WDW. Tumor target prostate specific membrane antigen (PSMA) and its regulation in prostate cancer. J Cell Biochem. 2004 Feb 15;91(3):528–39.

25. Basler M, Groettrup M. Advances in Prostate Cancer Immunotherapies. Drugs Aging. 2007 Mar 1;24(3):197–221.

26. Hoption Cann SA, van Netten JP, van Netten C. Dr William Coley and tumour regression: a place in history or in the future. Postgrad Med J. 2003 Dec;79(938):672–80.

27. Morse MA, Gwin WR, Mitchell DA. Vaccine Therapies for Cancer: Then and Now. Target Oncol. 2021 Mar 1;16(2):121–52.

28. Bou-Dargham MJ, Sha L, Sang QXA, Zhang J. Immune landscape of human prostate cancer: immune evasion mechanisms and biomarkers for personalized immunotherapy. BMC Cancer. 2020 Jun 18;20(1):572.

29. Mihalyo MA, Hagymasi AT, Slaiby AM, Nevius EE, Adler AJ. Dendritic cells program non-immunogenic prostate-specific T cell responses beginning at early stages of prostate tumorigenesis. The Prostate. 2007 Apr;67(5):536–46.

30. Troy A, Davidson P, Atkinson C, Hart D. Phenotypic characterisation of the dendritic cell infiltrate in prostate cancer. J Urol. 1998 Jul;160(1):214–9.

31. Collin M, Bigley V. Human dendritic cell subsets: an update. Immunology. 2018 May;154(1):3–20.

32. Steinman RM. Linking innate to adaptive immunity through dendritic cells. Novartis Found Symp. 2006;279:101–9; discussion 109-113, 216–9.

33. Fearnley DB, Whyte LF, Carnoutsos SA, Cook AH, Hart DN. Monitoring human blood dendritic cell numbers in normal individuals and in stem cell transplantation. Blood. 1999 Jan 15;93(2):728–36.

34. Sutherland SIM, Ju X, Horvath LG, Clark GJ. Moving on From Sipuleucel-T: New Dendritic Cell Vaccine Strategies for Prostate Cancer. Front Immunol. 2021 Mar 29;12:641307.

35. Sallusto F, Lanzavecchia A. Efficient presentation of soluble antigen by cultured human dendritic cells is maintained by granulocyte/macrophage colony-stimulating factor plus interleukin 4 and downregulated by tumor necrosis factor alpha. J Exp Med. 1994 Apr 1;179(4):1109–18.

36. Embgenbroich M, Burgdorf S. Current Concepts of Antigen Cross-Presentation. Front Immunol [Internet]. 2018 [cited 2022 May 18];9. Available from: https://www.frontiersin.org/article/10.3389/fimmu.2018.01643

37. Anassi E, Ndefo UA. Sipuleucel-T (Provenge) Injection. Pharm Ther. 2011 Apr;36(4):197–202.

38. Sheikh NA, Jones LA. CD54 is a surrogate marker of antigen presenting cell activation. Cancer Immunol Immunother. 2008 Sep 1;57(9):1381–90.

39. Kantoff PW, Higano CS, Shore ND, Berger ER, Small EJ, Penson DF, et al. Sipuleucel-T immunotherapy for castration-resistant prostate cancer. N Engl J Med. 2010 Jul 29;363(5):411–22.

40. Drake CG, Quinn D, Dreicer R, Antonarakis E, Shore N, Corman J, et al. Immune response from STRIDE, a randomized, Phase II, open-label study of sipuleucel-T (sip-T) with concurrent vs sequential enzalutamide (enz) administration in metastatic castration-resistant prostate cancer (mCRPC). J Immunother Cancer. 2015 Nov 4;3(Suppl 2):P145.

41. Madan RA, Antonarakis ES, Drake CG, Fong L, Yu EY, McNeel DG, et al. Putting the Pieces Together: Completing the Mechanism of Action Jigsaw for Sipuleucel-T. J Natl Cancer Inst. 2020 Jun 1;112(6):562–73.

42. Chen DS, Mellman I. Elements of cancer immunity and the cancer–immune set point. Nature. 2017 Jan;541(7637):321–30.

43. Concurrent, but not sequential, PD-1 blockade with a DNA vaccine elicits anti-tumor responses in patients with metastatic, castration-resistant prostate cancer - PubMed [Internet]. [cited 2022 Aug 10]. Available from: https://pubmed.ncbi.nlm.nih.gov/29876010/

44. Nelde A, Rammensee HG, Walz JS. The Peptide Vaccine of the Future. Mol Cell Proteomics [Internet]. 2021 Jan 1 [cited 2022 Aug 11];20. Available from: https://www.mcponline.org/article/S1535-9476(20)35136-7/abstract

45. Calvo Tardón M, Allard M, Dutoit V, Dietrich PY, Walker PR. Peptides as cancer vaccines. Curr Opin Pharmacol. 2019 Aug 1;47:20–6.

46. Skwarczynski M, Toth I. Peptide-based synthetic vaccines. Chem Sci. 2016 Feb 1;7(2):842–54.

47. How mRNA Vaccines Might Help Treat Cancer - NCI [Internet]. 2022 [cited 2022 Aug 11]. Available from: https://www.cancer.gov/news-events/cancer-currents-blog/2022/mrna-vaccines-to-treat-cancer

48. Kongsted P, Borch TH, Ellebaek E, Iversen TZ, Andersen R, Met Ö, et al. Dendritic cell vaccination in combination with docetaxel for patients with metastatic castration-resistant prostate cancer: A randomized phase II study. Cytotherapy. 2017 Apr;19(4):500–13.

49. Huang LM and YZ and L. mRNA vaccine for cancer immunotherapy | EndNote Click [Internet]. [cited 2022 Aug 11]. Available from: https://click.endnote.com/viewer?doi=10.1186%2Fs12943-021-01335-5&token=WzM0ODM0NTIsIjEwLjExODYvczEyOTQzLTAyMS0wMTMzNS01Il0.mzO8nwV2FR1j7j-G3XAMGFahxX8

50. Immune Checkpoint Inhibitors - NCI [Internet]. 2019 [cited 2022 Aug 10]. Available from: https://www.cancer.gov/about-cancer/treatment/types/immunotherapy/checkpoint-inhibitors

51. Frontiers | PD-1 and PD-L1 Checkpoint Signaling Inhibition for Cancer Immunotherapy: Mechanism, Combinations, and Clinical Outcome [Internet]. [cited 2022 Aug 10]. Available from: https://www.frontiersin.org/articles/10.3389/fphar.2017.00561/full

52. Park JA, Cheung NKV. Limitations and opportunities for immune checkpoint inhibitors in pediatric malignancies. Cancer Treat Rev. 2017 Jul;58:22–33.

53. Kwon ED, Drake CG, Scher HI, Fizazi K, Bossi A, van den Eertwegh AJM, et al. Ipilimumab versus placebo after radiotherapy in patients with metastatic castration-resistant prostate cancer that had progressed after docetaxel chemotherapy (CA184-043): a multicentre, randomised, double-blind, phase 3 trial. Lancet Oncol. 2014 Jun;15(7):700–12.

54. CAR T Cells: Engineering Immune Cells to Treat Cancer - NCI [Internet]. 2013 [cited 2022 Aug 10]. Available from: https://www.cancer.gov/about-cancer/treatment/research/car-t-cells

55. Tschernia NP, Norberg SM, Gulley JL. CAR T cells reach clinical milestone in prostate cancer. Nat Med. 2022 Apr;28(4):635–6.

56. Greene KL, Albertsen PC, Babaian RJ, Carter HB, Gann PH, Han M, et al. Prostate Specific Antigen Best Practice Statement: 2009 Update. J Urol. 2013 Spring;189(1, Supplement):S2–11.

57. Vickers AJ. Prostate Cancer Screening: Time to Question How to Optimize the Ratio of Benefits and Harms. Ann Intern Med. 2017 Oct 3;167(7):509–10.

58. Moradi A, Srinivasan S, Clements J, Batra J. Beyond the biomarker role: prostate-specific antigen (PSA) in the prostate cancer microenvironment. Cancer Metastasis Rev. 2019 Sep 1;38(3):333–46.

59. Pampalakis G, Sotiropoulou G. Tissue kallikrein proteolytic cascade pathways in normal physiology and cancer. Biochim Biophys Acta. 2007 Sep;1776(1):22–31.

60. Gorelik L, Flavell RA. Immune-mediated eradication of tumors through the blockade of transforming growth factor-β signaling in T cells. Nat Med. 2001 Oct;7(10):1118–22.

61. Kiessling A, Wehner R, Füssel S, Bachmann M, Wirth MP, Schmitz M. Tumor-Associated Antigens for Specific Immunotherapy of Prostate Cancer. Cancers. 2012 Mar;4(1):193–217.

62. Geary SM, Lemke CD, Lubaroff DM, Salem AK. Proposed mechanisms of action for prostate cancer vaccines. Nat Rev Urol. 2013 Mar 1;10(3):149–61.

63. Gulley JL, Heery CR, Madan RA, Walter BA, Merino MJ, Dahut WL, et al. Phase I study of intraprostatic vaccine administration in men with locally recurrent or progressive prostate cancer. Cancer Immunol Immunother CII. 2013 Sep;62(9):1521–31.

64. Kantoff PW, Schuetz TJ, Blumenstein BA, Glode LM, Bilhartz DL, Wyand M, et al. Overall Survival Analysis of a Phase II Randomized Controlled Trial of a Poxviral-Based PSA-Targeted Immunotherapy in Metastatic Castration-Resistant Prostate Cancer. J Clin Oncol. 2010 Mar 1;28(7):1099–105.

65. Gulley JL, Borre M, Vogelzang NJ, Ng S, Agarwal N, Parker CC, et al. Phase III Trial of PROSTVAC in Asymptomatic or Minimally Symptomatic Metastatic Castration-Resistant Prostate Cancer. J Clin Oncol Off J Am Soc Clin Oncol. 2019 May 1;37(13):1051–61.

66. Madan RA, Karzai F, Donahue RN, Al-Harthy M, Bilusic M, Rosner II, et al. Clinical and immunologic impact of short-course enzalutamide alone and with immunotherapy in non-metastatic castration sensitive prostate cancer. J Immunother Cancer. 2021 Mar;9(3):e001556.

67. Fong L. An Open Label, Randomized Phase 2 Trial of Prostvac and Ipilimumab as Monotherapy or in Combination for Men With Localized Prostate Cancer Undergoing Radical Prostatectomy [Internet]. clinicaltrials.gov; 2021 Oct [cited 2022 Aug 11]. Report No.: results/NCT02506114. Available from: https://clinicaltrials.gov/ct2/show/results/NCT02506114

68. Washington University School of Medicine. A Pilot Trial of Neoantigen DNA Vaccine in Combination With Nivolumab/Ipilimumab and PROSTVAC in Metastatic Hormone-Sensitive Prostate Cancer [Internet]. clinicaltrials.gov; 2022 Aug [cited 2022 Aug 11]. Report No.: results/NCT03532217. Available from: https://clinicaltrials.gov/ct2/show/results/NCT03532217

69. Couture A, Garnier A, Docagne F, Boyer O, Vivien D, Le-Mauff B, et al. HLA-Class II Artificial Antigen Presenting Cells in CD4+ T Cell-Based Immunotherapy. Front Immunol [Internet]. 2019 [cited 2022 Aug 16];10. Available from: https://www.frontiersin.org/articles/10.3389/fimmu.2019.01081

70. Riese RJ, Mitchell RN, Villadangos JA, Shi GP, Palmer JT, Karp ER, et al. Cathepsin S activity regulates antigen presentation and immunity. [Internet]. American Society for Clinical Investigation; 1998 [cited 2022 Aug 16]. Available from: https://www.jci.org/articles/view/1158/pdf

71. Wieczorek M, Abualrous ET, Sticht J, Álvaro-Benito M, Stolzenberg S, Noé F, et al. Major Histocompatibility Complex (MHC) Class I and MHC Class II Proteins: Conformational Plasticity in Antigen Presentation. Front Immunol [Internet]. 2017 [cited 2022 Aug 16];8. Available from: https://www.frontiersin.org/articles/10.3389/fimmu.2017.00292

72. Cai L, Zhang J, Zhu R, Shi W, Xia X, Edwards M, et al. Protective cellular immunity generated by cross-presenting recombinant overlapping peptide proteins. Oncotarget. 2017 Sep 29;8(44):76516–24.

73. Duan L, Mukherjee E. Janeway's Immunobiology, Ninth Edition. Yale J Biol Med. 2016 Sep 30;89(3):424–5.

74. Zhang H, Hong H, Li D, Ma S, Di Y, Stoten A, et al. Comparing Pooled Peptides with Intact Protein for Accessing Cross-presentation Pathways for Protective CD8+ and CD4+ T Cells *. J Biol Chem. 2009 Apr 3;284(14):9184–91.

75. Shen L, Sigal LJ, Boes M, Rock KL. Important role of cathepsin S in generating peptides for TAP-independent MHC class I crosspresentation in vivo. Immunity. 2004 Aug;21(2):155–65.

76. Joffre OP, Segura E, Savina A, Amigorena S. Cross-presentation by dendritic cells. Nat Rev Immunol. 2012 Aug;12(8):557–69.

77. Kovacsovics-Bankowski M, Rock KL. A phagosome-to-cytosol pathway for exogenous antigens presented on MHC class I molecules. Science. 1995 Jan 13;267(5195):243–6.

78. Guermonprez P, Saveanu L, Kleijmeer M, Davoust J, Van Endert P, Amigorena S. ER-phagosome fusion defines an MHC class I cross-presentation compartment in dendritic cells. Nature. 2003 Sep 25;425(6956):397–402.

79. Burgdorf S, Schölz C, Kautz A, Tampé R, Kurts C. Spatial and mechanistic separation of cross-presentation and endogenous antigen presentation. Nat Immunol. 2008 May;9(5):558–66.

80. Driessen C, Bryant RAR, Lennon-Duménil AM, Villadangos JA, Bryant PW, Shi GP, et al. Cathepsin S Controls the Trafficking and Maturation of Mhc Class II Molecules in Dendritic Cells. J Cell Biol. 1999 Nov 15;147(4):775–90.

81. Cai L, Zhang J, Zhu R, Shi W, Xia X, Edwards M, et al. Protective cellular immunity generated by cross-presenting recombinant overlapping peptide proteins. Oncotarget. 2017 Aug 24;8(44):76516–24.

82. Stephens AJ, Burgess-Brown NA, Jiang S. Beyond Just Peptide Antigens: The Complex World of Peptide-Based Cancer Vaccines. Front Immunol [Internet]. 2021 [cited 2022 Aug 17];12. Available from: https://www.frontiersin.org/articles/10.3389/fimmu.2021.696791

83. Dupuis M, Denis-Mize K, Woo C, Goldbeck C, Selby MJ, Chen M, et al. Distribution of DNA Vaccines Determines Their Immunogenicity After Intramuscular Injection in Mice. J Immunol. 2000 Sep 1;165(5):2850–8.

84. Hobernik D, Bros M. DNA Vaccines—How Far From Clinical Use? Int J Mol Sci. 2018 Nov;19(11):3605.

85. Miao L, Zhang Y, Huang L. mRNA vaccine for cancer immunotherapy. Mol Cancer. 2021 Feb 25;20(1):41.

86. Endotoxin Quantitation and Removal - UK [Internet]. [cited 2022 Aug 3]. Available from: https://www.thermofisher.com/uk/en/home/life-science/protein-biology/protein-purification-isolation/protein-purification/endotoxin-quantitation-removal.html

87. Pierce™ BCA Protein Assay Kit [Internet]. [cited 2022 Aug 3]. Available from: https://www.thermofisher.com/order/catalog/product/23225

88. Proteome Profiler Mouse Cytokine Array Kit, Panel A [Internet]. www.rndsystems.com. [cited 2022 Aug 7]. Available from: https://www.rndsystems.com/products/proteome-profiler-mouse-cytokine-array-kit-panel-a_ary006

89. Bhat EA, Abdalla M, Rather IA, Bhat EA, Abdalla M, Rather IA. Key Factors for Successful Protein Purification and Crystallization. Glob J Biotechnol Biomater Sci. 2018 Aug 10;4(1):001–7.

90. Wang SSS, Chang CK, Peng MJ, Liu HS. Effect of Glutathione Redox System on Lysozyme Refolding in Size Exclusion Chromatography. Food Bioprod Process. 2006 Mar 1;84(1):18–27.

91. Recombinant Human Cathepsin S Protein, HEK293 Cells, His Tag, 10487-H08H | Sino Biological [Internet]. [cited 2022 Sep 10]. Available from: https://www.sinobiological.com/recombinant-proteins/human-cathepsin-s-10487-h08h

92. KRT9 - Keratin, type I cytoskeletal 9 - Homo sapiens (Human) | UniProtKB | UniProt [Internet]. [cited 2022 Sep 9]. Available from: https://www.uniprot.org/uniprotkb/P35527/entry

93. Loiseau L, Gerez C, Bekker M, Ollagnier-de Choudens S, Py B, Sanakis Y, et al. ErpA, an iron sulfur (Fe S) protein of the A-type essential for respiratory metabolism in Escherichia coli. Proc Natl Acad Sci U S A. 2007 Aug 21;104(34):13626–31.

94. Martino L, He Y, Hands-Taylor KLD, Valentine ER, Kelly G, Giancola C, et al. The interaction of the Escherichia coli protein SlyD with nickel ions illuminates the mechanism of regulation of its peptidyl-prolyl isomerase activity. FEBS J. 2009 Aug;276(16):4529–44.

95. Das A, Mukhopadhyay C. Urea-Mediated Protein Denaturation: A Consensus View. J Phys Chem B. 2009 Sep 24;113(38):12816–24.

96. Upadhyay R. Re: Which one is better for protein denaturation Guanidine or Urea?. [Internet]. ResearchGate. 2015 [cited 2022 Aug 30]. Available from: https://www.researchgate.net/post/Which-one-is-better-for-protein-denaturation-Guanidine-or-Urea

97. Cromwell MEM, Hilario E, Jacobson F. Protein aggregation and bioprocessing. AAPS J. 2006 Sep 1;8(3):E572–9.

98. Ni-NTA Agarose [Internet]. [cited 2022 Aug 30]. Available from: https://www.qiagen.com/us/products/discovery-and-translational-research/protein-purification/tagged-protein-expression-purification-detection/ni-nta-agarose/

99. Rosano GL, Ceccarelli EA. Recombinant protein expression in Escherichia coli: advances and challenges. Front Microbiol [Internet]. 2014 [cited 2022 Aug 31];5. Available from: https://www.frontiersin.org/articles/10.3389/fmicb.2014.00172

100. HARTLEY DL, KANE JF. Properties of inclusion bodies from recombinant Escherichia coli. Biochem Soc Trans. 1988 Apr 1;16(2):101–2.

101. Carrió MM, Villaverde A. Construction and deconstruction of bacterial inclusion bodies. J Biotechnol. 2002 Jun 13;96(1):3–12.

102. Sørensen HP. Towards universal systems for recombinant gene expression. Microb Cell Factories. 2010 Apr 30;9(1):27.

103. Nielsen KH. Chapter Twelve - Protein Expression-Yeast. In: Lorsch J, editor. Methods in Enzymology [Internet]. Academic Press; 2014 [cited 2022 Aug 31]. p. 133–47. (Laboratory Methods in Enzymology: Protein Part A; vol. 536). Available from: https://www.sciencedirect.com/science/article/pii/B978012420070800012X

104. Bill R. Playing catch-up with Escherichia coli: using yeast to increase success rates in recombinant protein production experiments. Front Microbiol [Internet]. 2014 [cited 2022 Aug 31];5. Available from: https://www.frontiersin.org/articles/10.3389/fmicb.2014.00085

105. Khan KH. Gene Expression in Mammalian Cells and its Applications. Adv Pharm Bull. 2013 Dec;3(2):257–63.

106. Overview of Protein Expression Systems - UK [Internet]. [cited 2022 Aug 31]. Available from: https://www.thermofisher.com/uk/en/home/life-science/protein-biology/protein-biology-learning-center/protein-biology-resource-library/pierce-protein-methods/overview-protein-expression-systems.html

107. van Oers MM. Opportunities and challenges for the baculovirus expression system. J Invertebr Pathol. 2011 Jul 1;107:S3–15.

108. Wolfert MA, Boons GJ. Adaptive immune activation: glycosylation does matter. Nat Chem Biol. 2013 Dec;9(12):776–84.

109. Taylor ME, Drickamer K. Structure-function analysis of C-type animal lectins. Methods Enzymol. 2003;363:3–16.

110. Hanisch FG, Ninkovic T. Immunology of O-glycosylated proteins: approaches to the design of a MUC1 glycopeptide-based tumor vaccine. Curr Protein Pept Sci. 2006 Aug;7(4):307–15.

111. Jaffé SR, Strutton B, Levarski Z, Pandhal J, Wright PC. Escherichia coli as a glycoprotein production host: recent developments and challenges. Curr Opin Biotechnol. 2014 Dec 1;30:205–10.

112. Valderrama-Rincon JD, Fisher AC, Merritt JH, Fan YY, Reading CA, Chhiba K, et al. An engineered eukaryotic protein glycosylation pathway in Escherichia coli. Nat Chem Biol. 2012 May;8(5):434–6.

113. Pandhal J, Woodruff LBA, Jaffe S, Desai P, Ow SY, Noirel J, et al. Inverse metabolic engineering to improve Escherichia coli as an N-glycosylation host. Biotechnol Bioeng. 2013;110(9):2482–93.

114. Trimpin S, Brizzard B. Analysis of insoluble proteins. BioTechniques. 2009 May;46(6):409–19.

115. Costa S, Almeida A, Castro A, Domingues L. Fusion tags for protein solubility, purification and immunogenicity in Escherichia coli: the novel Fh8 system. Front Microbiol. 2014 Feb 19;5:63.

116. Sørensen HP, Mortensen KK. Soluble expression of recombinant proteins in the cytoplasm of Escherichia coli. Microb Cell Factories. 2005 Jan 4;4(1):1.

117. Nickel Columns and Nickel Resin | Bio-Rad [Internet]. [cited 2022 Aug 30]. Available from: https://www.bio-rad.com/featured/en/nickel-columns-nickel-resin.html

118. Optimizing Purification of Histidine-Tagged Proteins [Internet]. [cited 2022 Aug 30]. Available from: https://www.sigmaaldrich.com/GB/en/technical-documents/technical-article/protein-biology/protein-purification/optimizing-purification-of-histidine-tagged-proteins

119. Troubleshooting Guide for Affinity Chromatography of Tagged Proteins [Internet]. [cited 2022 Sep 5]. Available from: https://www.sigmaaldrich.com/GB/en/technical-documents/technical-article/protein-biology/protein-purification/troubleshooting1

120. Ariza A. Re: Can I use EDTA and/or DTT in wash buffer and elution buffer used for Ni affinity chromatography? [Internet]. ResearchGate. 2014 [cited 2022 Sep 5]. Available from: https://www.researchgate.net/post/Can_I_use_EDTA_and_or_DTT_in_wash_buffer_and_elution_buffer_used_for_Ni_affinity_chromatography/541960c0d2fd6411448b45cd/citation/download.

121. Yamaguchi H, Miyazaki M. Refolding Techniques for Recovering Biologically Active Recombinant Proteins from Inclusion Bodies. Biomolecules. 2014 Feb 20;4(1):235–51.

122. Playter G. Approaches to Scaling Up Chromatography Processes. BioPharm Int. 2022 Sep 2;27(9):26–7.

123. Webster GK, Chang JC, Heflin JL. Stability Indicating Method for Polysorbate 80 in Protein Formulations. J Chromatogr Sci. 2021 Aug 18;59(8):706–13.

124. Sun H, Yang R, Wang J, Yang X, Tu J, Xie L, et al. Component-based biocompatibility and safety evaluation of polysorbate 80. RSC Adv. 2017;7(25):15127–38.

125. Thibeault J, Patrick J, Martin A, Ortiz-Perez B, Hill S, Zhang S, et al. Sarkosyl: A milder detergent than SDS for identifying proteins with moderately high hyperstability using gel electrophoresis. Anal Biochem. 2019 Apr 15;571:21–4.

126. Suppression of protein interactions by arginine: A proposed mechanism of the arginine effects - ScienceDirect [Internet]. [cited 2022 Sep 6]. Available from: https://www.sciencedirect.com/science/article/abs/pii/S0301462206003462

127. Tischer A, Lilie H, Rudolph R, Lange C. L-Arginine hydrochloride increases the solubility of folded and unfolded recombinant plasminogen activator rPA. Protein Sci. 2010;19(9):1783–95.

128. Thomson CA, Olson M, Jackson LM, Schrader JW. A Simplified Method for the Efficient Refolding and Purification of Recombinant Human GM-CSF. PLOS ONE. 2012 Nov 14;7(11):e49891.

129. Cao E, Chen Y, Cui Z, Foster PR. Effect of freezing and thawing rates on denaturation of proteins in aqueous solutions. Biotechnol Bioeng. 2003 Jun 20;82(6):684–90.

130. Tjernberg A, Markova N, Griffiths WJ, Hallén D. DMSO-related effects in protein characterization. J Biomol Screen. 2006 Mar;11(2):131–7.

131. Arango Duque G, Descoteaux A. Macrophage Cytokines: Involvement in Immunity and Infectious Diseases. Front Immunol [Internet]. 2014 [cited 2022 Sep 7];5. Available from: https://www.frontiersin.org/articles/10.3389/fimmu.2014.00491

132. Blanco P, Palucka AK, Pascual V, Banchereau J. Dendritic cells and cytokines in human inflammatory and autoimmune diseases. Cytokine Growth Factor Rev. 2008 Feb;19(1):41–52.

133. Shen Z, Reznikoff G, Dranoff G, Rock KL. Cloned dendritic cells can present exogenous antigens on both MHC class I and class II molecules. J Immunol Baltim Md 1950. 1997 Mar 15;158(6):2723–30.

134. Anderson DA, Dutertre CA, Ginhoux F, Murphy KM. Genetic models of human and mouse dendritic cell development and function. Nat Rev Immunol. 2021 Feb;21(2):101–15.

135. Shortman K, Liu YJ. Mouse and human dendritic cell subtypes. Nat Rev Immunol. 2002 Mar;2(3):151–61.

136. Banchereau J, Steinman RM. Dendritic cells and the control of immunity. Nature. 1998 Mar;392(6673):245–52.

137. Mehta AK, Gracias DT, Croft M. TNF activity and T cells. Cytokine. 2018 Jan 1;101:14–8.

138. Sheikh N, Jones LA. CD54 is a surrogate marker of antigen presenting cell activation. Cancer Immunol Immunother CII. 2008 Oct 1;57:1381–90.

139. Castellino F, Huang AY, Altan-Bonnet G, Stoll S, Scheinecker C, Germain RN. Chemokines enhance immunity by guiding naive CD8+ T cells to sites of CD4+ T cell-dendritic cell interaction. Nature. 2006 Apr 13;440(7086):890–5.

140. Thaiss C, Semmling V, Franken L, Wagner H, Kurts C. Chemokines: A New Dendritic Cell Signal for T Cell Activation. Front Immunol [Internet]. 2011 [cited 2022 Sep 7];2. Available from: https://www.frontiersin.org/articles/10.3389/fimmu.2011.00031

141. Tahtinen S, Tong AJ, Himmels P, Oh J, Paler-Martinez A, Kim L, et al. IL-1 and IL-1ra are key regulators of the inflammatory response to RNA vaccines. Nat Immunol. 2022 Apr;23(4):532–42.

142. Kranz LM, Diken M, Haas H, Kreiter S, Loquai C, Reuter KC, et al. Systemic RNA delivery to dendritic cells exploits antiviral defence for cancer immunotherapy. Nature. 2016 Jun;534(7607):396–401.

143. Farhood B, Najafi M, Mortezaee K. CD8+ cytotoxic T lymphocytes in cancer immunotherapy: A review. J Cell Physiol. 2019 Jun;234(6):8509–21.

144. Borst J, Ahrends T, Bąbała N, Melief CJM, Kastenmüller W. CD4+ T cell help in cancer immunology and immunotherapy. Nat Rev Immunol. 2018 Oct;18(10):635–47.

145. Tay RE, Richardson EK, Toh HC. Revisiting the role of CD4+ T cells in cancer immunotherapy-new insights into old paradigms. Cancer Gene Ther. 2021 Feb;28(1–2):5–17.

146. Schoenberger SP, Toes RE, van der Voort EI, Offringa R, Melief CJ. T-cell help for cytotoxic T lymphocytes is mediated by CD40-CD40L interactions. Nature. 1998 Jun 4;393(6684):480–3.

147. Bennett SR, Carbone FR, Karamalis F, Flavell RA, Miller JF, Heath WR. Help for cytotoxic-T-cell responses is mediated by CD40 signalling. Nature. 1998 Jun 4;393(6684):478–80.

148. Kennedy R, Celis E. Multiple roles for CD4+ T cells in anti-tumor immune responses. Immunol Rev. 2008 Apr;222(1):129–44.

149. Sidney J, del Guercio MF, Southwood S, Engelhard VH, Appella E, Rammensee HG, et al. Several HLA alleles share overlapping peptide specificities. J Immunol Baltim Md 1950. 1995 Jan 1;154(1):247–59.

150. Di L. Strategic approaches to optimizing peptide ADME properties. AAPS J. 2015 Jan;17(1):134–43.

151. Bijker MS, van den Eeden SJF, Franken KL, Melief CJM, van der Burg SH, Offringa R. Superior induction of anti-tumor CTL immunity by extended peptide vaccines involves prolonged, DC-focused antigen presentation. Eur J Immunol. 2008;38(4):1033–42.

152. Rosalia RA, Quakkelaar ED, Redeker A, Khan S, Camps M, Drijfhout JW, et al. Dendritic cells process synthetic long peptides better than whole protein, improving antigen presentation and T-cell activation. Eur J Immunol. 2013 Oct;43(10):2554–65.

153. Rabu C, Rangan L, Florenceau L, Fortun A, Charpentier M, Dupré E, et al. Cancer vaccines: designing artificial synthetic long peptides to improve presentation of class I and class II T cell epitopes by dendritic cells. Oncoimmunology. 2019 Jan 17;8(4):e1560919.

154. Oxford Vacmedix UK Ltd. A Phase 1, Multicentre, Open-label, Nonrandomised, First-in-human Study of OVM-200 as a Therapeutic Vaccine in Patients With Locally Advanced or Metastatic Non-Small Cell Lung Cancer, Ovarian Cancer, and Prostate Cancer [Internet]. clinicaltrials.gov; 2022 Apr [cited 2022 Sep 7]. Report No.: NCT05104515. Available from: https://clinicaltrials.gov/ct2/show/NCT05104515

155. Legat A, Maby-El Hajjami H, Baumgaertner P, Cagnon L, Abed Maillard S, Geldhof C, et al. Vaccination with LAG-3Ig (IMP321) and Peptides Induces Specific CD4 and CD8 T-Cell Responses in Metastatic Melanoma Patients--Report of a Phase I/IIa Clinical Trial. Clin Cancer Res Off J Am Assoc Cancer Res. 2016 Mar 15;22(6):1330–40.

156. Rausch S, Gouttefangeas C, Hennenlotter J, Laske K, Walter K, Feyerabend S, et al. Results of a Phase 1/2 Study in Metastatic Renal Cell Carcinoma Patients Treated with a Patient-specific Adjuvant Multi-peptide Vaccine after Resection of Metastases. Eur Urol Focus. 2019 Jul 1;5(4):604–7.

157. TLR activation triggers the rapid differentiation of monocytes into macrophages and dendritic cells | Nature Medicine [Internet]. [cited 2022 Aug 17]. Available from: https://www.nature.com/articles/nm1246

158. Kano Y, Iguchi T, Matsui H, Adachi K, Sakoda Y, Miyakawa T, et al. Combined adjuvants of poly(I:C) plus LAG-3-Ig improve antitumor effects of tumor-specific T cells, preventing their exhaustion. Cancer Sci. 2016 Apr;107(4):398–406.

159. Boks MA, Bruijns SCM, Ambrosini M, Kalay H, Bloois L van, Storm G, et al. In situ Delivery of Tumor Antigen– and Adjuvant-Loaded Liposomes Boosts Antigen-Specific T-Cell Responses by Human Dermal Dendritic Cells. J Invest Dermatol. 2015 Nov 1;135(11):2697–704.

160. Beutler B, Rietschel ET. Innate immune sensing and its roots: the story of endotoxin. Nat Rev Immunol. 2003 Feb;3(2):169–76.

161. Rastakhiz S, Yazdani M, Shariat S, Arab A, Momtazi-Borojeni AA, Barati N, et al. Preparation of nanoliposomes linked to HER2/neu-derived (P5) peptide containing MPL adjuvant as vaccine against breast cancer. J Cell Biochem. 2019 Feb;120(2):1294–303.

162. Wang YQ, Bazin-Lee H, Evans JT, Casella CR, Mitchell TC. MPL Adjuvant Contains Competitive Antagonists of Human TLR4. Front Immunol [Internet]. 2020 [cited 2022 Aug 17];11. Available from: https://www.frontiersin.org/articles/10.3389/fimmu.2020.577823

163. Duan Q, Zhang H, Zheng J, Zhang L. Turning Cold into Hot: Firing up the Tumor Microenvironment. Trends Cancer. 2020 Jul 1;6(7):605–18.

164. Grimaldi A, Cammarata I, Martire C, Focaccetti C, Piconese S, Buccilli M, et al. Combination of chemotherapy and PD-1 blockade induces T cell responses to tumor non-mutated neoantigens. Commun Biol. 2020 Feb 25;3(1):1–13.

165. Bailly C, Thuru X, Quesnel B. Combined cytotoxic chemotherapy and immunotherapy of cancer: modern times. NAR Cancer. 2020 Mar 1;2(1):zcaa002.

166. Roselli M, Cereda V, di Bari MG, Formica V, Spila A, Jochems C, et al. Effects of conventional therapeutic interventions on the number and function of regulatory T cells. Oncoimmunology. 2013 Oct 1;2(10):e27025.

167. Mixed 20-peptide cancer vaccine in combination with docetaxel and dexamethasone for castration-resistant prostate cancer: a randomized phase II trial - PubMed [Internet]. [cited 2022 Aug 17]. Available from: https://pubmed.ncbi.nlm.nih.gov/32025848/

168. Zhang Z, Lu M, Qin Y, Gao W, Tao L, Su W, et al. Neoantigen: A New Breakthrough in Tumor Immunotherapy. Front Immunol [Internet]. 2021 [cited 2022 Sep 9];12. Available from: https://www.frontiersin.org/articles/10.3389/fimmu.2021.672356